AN ABSTRACT OF THE DISSERTATION OF

Kevin Marley for the degree of
Doctor of Philosophy in Exercise and Sport Science
Presented on June 8, 2004.
Title: Skeletal Muscle Proteolysis after Fatigue and Exercise-Induced Injury.

Redacted for privacy

Abstract approved:

Jeffrey J. Widrick

Skeletal muscle damage induced by lengthening ("eccentric" or "pliometric") contractions cause an immediate loss in maximal tetanic force (P_o) and an increase in protein degradation by unidentified endogenous mechanisms. We hypothesized that increased proteolysis following active lengthening injury is mediated by the Ca^{2+} dependent protease calpain. To test this hypothesis we constructed an apparatus capable of inducing lengthening-contraction injury in rat extensor digitorum longus (EDL) and measured the calpain-specific proteolysis of α-fodrin in muscles subjected to either 90 *in-situ* active lengthening contractions (17.4 ± 0.3% of fiber length), 90 active isometric contractions, 90 passive lengthening contractions (18.4 ± 0.1% of fiber length) or no contractile treatment. Sixty minutes after the exercise treatments, isometric force had declined 4 ± 2% of

P_o in the isometric-contraction-treated muscles (n = 6), 4 ±1% in the passive-lengthening treatment (n = 3), and 5 ±3% in muscles that received no treatment other than isometric test contractures (n = 3). In contrast, force declined 53 ± 3% of P_o ($P < 0.01$ vs. all other treatments) in muscles subjected to active lengthening contractions (n = 6). Calpain-mediated fodrinolysis produces 145 kDa and 150 kDa peptides that retain immunoreactivity to the intact α-fodrin antibody. Densitometric analysis of α-fodrin Western blots showed that levels of these peptides were not different between the active isometric, passive lengthening, no treatment or contralateral muscle groups. In contrast, levels of the 145 kDa and 150 kDa peptides in muscles subjected to lengthening contractions were 5.75-fold greater ($P < 0.01$) than the combined mean of the non-injury treatments and 8.5-fold greater than contralateral muscles ($P < 0.01$). These data indicate that calpain-mediated proteolysis is increased following *in situ* lengthening contraction-induced injury in rat EDL muscles.

Skeletal Muscle Proteolysis after Fatigue and Exercise-Induced Injury

by

Kevin Marley

A DISSERTATION

submitted to

Oregon State University

in partial fulfillment of
the requirements for the
degree of

Doctor of Philosophy

Presented June 8, 2004
Commencement June 2005

Doctor of Philosophy dissertation of Kevin Marley
presented on June 8, 2004.

APPROVED: Redacted for privacy

Major Professor, representing Exercise and Sport Science

Redacted for privacy

Chair of the Department of Exercise and Sport Science

Redacted for privacy

Dean of the Graduate School

I understand that my dissertation will become part of the permanent collection of Oregon State University libraries. My signature below authorizes release of my dissertation to any reader upon request.

Redacted for privacy

Kevin Marley, Author

ACKNOWLEDGEMENTS

I feel it is important to acknowledge the fact that a number of living beings where killed in the course of this study. I am grateful to have been able to develop as a scientist at the expense of these animals lives and I am confident that the advancement of science makes this a worthwhile but not insignificant sacrifice.

I would like to thank my wife and best friend Giovanna Rosenlicht whose everlasting support made this possible. Giovanna has given me a wonderful example of perseverance and moral fortitude; her support has encompassed many forms but has always been encouraging, loving and enabling. Thank you!

Lastly, and in the spirit of tribute, I want to acknowledge my son, Jesse Marley, who through no intention of his own has given me a new perspective on what is important in life.

CONTRIBUTION OF AUTHORS

Dr. Forsberg assisted with the theoretical design of the calpain experiments.

Dr. Widrick assisted with the design and implementation of all aspects of this work.

TABLE OF CONTENTS

TABLE OF CONTENTS (continued)

Page

TABLE OF CONTENTS (continued)

TABLE OF CONTENTS (continued)

LIST OF FIGURES AND TABLES

Skeletal Muscle Proteolysis after Fatigue and Exercise-Induced Injury

Chapter 1

Introduction

Kevin Marley

Department of Exercise and Sport Science

Exercise Injury in Skeletal Muscle

1.1. Introduction

Musculoskeletal injuries in the United States account for nearly 70 million physician office visits and an annual economic burden estimated to approach $215 billion (16). Currently no comprehensive data exist that differentiate between types of injuries or identify whether they occur most often in occupational or recreational settings. Regardless of cause, evidence suggests that injury to skeletal muscle has a significant impact on economic, health, and quality of life indices in the United States (16). Nearly everyone has experienced the delayed onset muscle soreness and eventual recovery that occurs after unaccustomed or strenuous exercise, yet the biological processes that underlie these responses are not well understood. The purpose of this work was to examine one aspect of this response, calpain-mediated proteolysis, in exercise-injured skeletal muscle.

There are many unanswered questions concerning the injuries that occur when muscles repeatedly resist their own lengthening (termed lengthening, isometric, or pliometric contractions). These injuries cause an immediate, but transient, reduction in performance (43), and are associated with a number of clinical signs which include leakage of muscle proteins into the systemic circulation (92), disruption of sarcomere structure (89), tissue swelling, inflammation and reduced range of motion. An immediate decline in maximal force capacity of 50% or more is not uncommon (52). In severe cases, functional capacity may continue to decline for 72 hours post-injury (88, 100, 147). The

mechanism responsible for this post-injury decline in force has been hypothesized to result from the activation of autogenic (intrinsic) proteolytic mechanisms (8). One candidate for this mechanism is the selective and limited hydrolysis of muscle proteins by calpain (86).

The calpains are a family of endogenous calcium-activated neutral cysteine proteases. Their role in skeletal muscle response to injury is thought to be part of a cascade of events that ultimately result in recovery and transient protection from similar injury. Although there has been considerable scientific interest in elucidating the role of calpain function in skeletal muscle, the mechanism of their activation and their functional purpose remains poorly understood.

The purpose of this study was to measure the products of the *in vivo* calpain-mediated proteolysis of α-fodrin (an intermediate filament protein) following lengthening-induced muscle injury or damage. We hypothesized that calpains are activated following muscle damage. To test this hypothesis we evaluated the *in vivo* degradation of α-fodrin (or αII-spectrin), a well-characterized marker of calpain-mediated proteolysis (69, 121, 146), in rat extensor digitorum longus muscles (EDL) injured by lengthening contractions.

Chapter 2

Literature Review

2.1. Introduction

Lengthening contractions are those where muscles absorb energy by actively opposing their own lengthening. These types of contractions occur during both recreational and occupational activities that involve deceleration of internal or external mass. These are used in braking, turning and lowering maneuvers. It has been well established that lengthening contractions cause muscle injury, but the mechanisms responsible for injury are a matter of debate. These lengthening contraction-induced (also called exercise-induced) injuries are associated with sarcomere disruption (47), a shift in the length-tension relation (77), muscle protein efflux into the systemic circulation (129), prolonged muscle dysfunction (153), delayed onset muscle soreness, and ultimately adaptation and transient protection from similar injury (126).

Light and electron micrographs of exercise-damaged tissue often show structural alterations observed immediately and for up to 7 days post-injury (106, 108). Common observations of damage include Z-lines that are out of register, degraded or missing altogether, disrupted M-line structure, and the appearance of hyper-contracted or overextended sarcomeres (52). This ultrastructural damage is postulated to also create ruptures in the sarcolema, which then allow ion (Ca^{2+}, and Na^{+}) influx and leakage of muscle enzymes into the systemic circulation (134).

There are a number of muscle proteins, peptides, and amino acids that appear in plasma after exercise injury and are used as markers of muscle injury. These include creatine kinase, lactate dehydrogenase, tyrosine, and myosin peptides (129). Methylhistidine, a product of muscle protein degradation, may appear in urine after exercise and is also sometimes used as marker of muscle injury (111). The appearance of one or more of these markers after exercise gives evidence of muscle injury (50), but it is important to note that the magnitude of these markers is also a function of their clearance and may additionally be affected by systemic hydration levels (34). As a result, these indices of muscle damage may be unreliable. Ultrastructural damage and muscle protein efflux after exercise should be considered supportive, but not direct, evidence of muscle damage because they are often poorly correlated with the loss in function seen in injured tissue (24).

Commonly reported parameters of isolated muscle function include peak twitch force (P_t), time to peak force, ½ relaxation time and peak tetanic force (P_o). These variables are obtained isometrically (no change in muscle length) at optimal length (L_o). A lasting decline in P_o is the most commonly reported and well-accepted marker of muscle damage (153). The magnitude of this loss ranges between 25 and 33% in human models (52, 156) and commonly exceeds 50% in animal models (14, 33, 92). Most evidence supports the hypothesis that this force deficit arises due to a combination of disruption of actin and myosin filaments and impairment in one or more mechanisms of excitation contraction coupling (EC-

coupling), a term used to describe membrane excitation, calcium release, and reuptake by the sarcoplasmic reticulum (SR) (48).

Mechanisms of EC-coupling can be bypassed with the use of caffeine in single skinned muscle fibers or whole muscles. Caffeine causes Ca^{2+} channels in the SR to open and results in partial restoration of the loss in force observed after muscle injury (71). Similarly, the drug 4-Chloro-m-cresol can be used to by-pass EC-coupling in intact muscles. Ingalls et al. (71) used 4-Chloro-m-cresol in lengthening-contraction-injured mouse EDL and attributed 57-75% of P_o decrement to disrupted EC-coupling. Thus it seems reasonable to attribute failure of mechanisms of EC-coupling to a significant portion of the force loss after exercise-injury, but evidence suggests that changes in other mechanisms are also involved, such as a shift in the length-tension relation.

In this regard, Katz (77) first reported a shift in the length-tension relation to longer sarcomere lengths after injury, an observation that has since been confirmed (for review see ref (102)). This has been interpreted to suggest that some sarcomeres become overextended during lengthening contractions. While these overextended sarcomeres normally reinterdigitate during muscle shortening, it has been hypothesized that repeated stretches result in the failure of some sarcomeres to reinterdigitate and damage to the muscle fiber (102). This idea will be covered in detail in section 2.3.3.

The delayed-onset muscle soreness (DOMS) that follows an injury usually increases in severity over the initial 24-72 hours after exercise, then declines and is

gone within 5-7 days (47). The severity of DOMS ranges from mild to debilitating. It has been proposed that severe cases of DOMS result in exertional rabdomyolosis but in most cases the symptoms are temporary and result in nothing more serious than mild discomfort (6). In fact, a protective effect often follows DOMS and limits future damage caused by similar activities (107).

This phenomenon, which is referred to as the repeated bout effect, occurs after as little as one sub-maximal bout of exercise and may confer protection for up to 6 months (107). There are a number of hypotheses that attempt to explain the mechanism for the repeated bout effect. These include a possible shift in recruitment patterns (99), an increase in the number sarcomeres in series (115) and a change in intermediate filaments such as desmin (15). It therefore seems reasonable that the repeated bout effect results from a combination of the above or some as yet undiscovered mechanism, and that this response depends on the type and magnitude of the initial stimulus.

2.2. Mechanisms of Muscle Injury

The causes and biological consequences that result from exercise-induced injury in skeletal muscle can be divided into the following 5 hypothetical stages: 1) an event causes the initial injury; 2) the cell can no longer maintain calcium homeostasis resulting in an increase in intracellular calcium concentration [Ca^{2+}]; 3) intrinsic, or autogenic, proteolytic mechanisms are activated; 4) phagocytes infiltrate the damaged tissue, and 5) regeneration and recovery (for reviews see 8,

19, 69). The purpose of this work is to investigate whether calpains participate in the autogenic phase. Consequently, this review will cover events leading up to and including the autogenic phase (stage 3).

2.3. The Initial Event in Muscle Injury

Hypothesized mechanisms of exercise injury in skeletal muscle can be described as those that are mechanical or those that are related to the byproducts of energy metabolism. Proposed metabolic mechanisms include acidosis, high temperature, insufficient mitochondrial respiration, and oxidative damage from free radicals. It has been well established that lengthening contractions cause more damage than either shortening or isometric contractions (15, 47, 48, 50, 71, 89, 115, 129). Since shortening and isometric contractions involve considerably more metabolic activity, it seems unlikely that metabolic mechanisms are responsible for the initial event. Thus, it has been hypothesized that one or more mechanical aspects of lengthening contractions are responsible for the initial injury. These mechanical factors include high force (stress), high strain (change in length) and inhomogeneity of sarcomere length. Each of these will be considered in detail below.

2.3.1 High Force as the Initiating Event

The most obvious factor that differentiates lengthening contractions from isometric or concentric contractions is the high specific force, e.g. the force per

cross-sectional area (CSA) of active tissue undergoing lengthening contractions. This can occur under conditions where net force is not different between contractile conditions (e.g. lengthening versus isometric contractions), because lengthening contractions are thought to recruit fewer muscle fibers to produce the same force (41). Combined, this evidence demonstrates that force/CSA of active muscle is high during lengthening contractions, but there are unanswered questions concerning the source of this increase in force and whether or not high force alone is responsible for injury in skeletal muscle.

During lengthening contractions, the ascending limb of the length-tension relation reflects increasing active tension with increasing sarcomere length. Active tension plateaus as actin and myosin filaments achieve optimal overlap, whereupon further lengthening results in a decline in active force but a concomitant increase in passive tension. In relatively noncompliant muscles (those that produce high passive tension with stretch), passive tension will increase at a rate such that total tension increases with continued stretch. More compliant tissues will show a dip in total force where the decline in active tension at longer than optimal sarcomere lengths is not made up by passive forces. Although this passive tension was initially thought to result entirely from connective tissue (32, 66), there are currently several hypotheses that suggest it is at least partially derived from intracellular components (65, 95). One such candidate thought to be responsible for several aspects of passive tension in skeletal muscle is the giant filamentous protein titin.

In the sarcomere, titin (also known as connectin) spans the distance from the Z-line to the M-line. Its mechanical properties are primarily responsible for the force that is generated during passive lengthening (150). In addition, titin is credited with restoring stretched sarcomeres to their slack length, maintaining A-bands in their central position during contraction, and limiting length inhomogeneity in series-linked sarcomeres (67). The I-band region contains immunoglobin-like (Ig) and praline, glutamate, valine, and lysine-rich (PEVK) domains that are proposed to have stiff and compliant spring properties respectively (145). The recent development of sequence-specific antibodies to titin resulted in the discovery that passive force is low and Ig domain unfolding predominates during stretches where sarcomere length remains below 2.7 μm. In contrast, during active-stretch conditions where sarcomere lengths range between 2.7 and 4.0 μm, passive force increases dramatically and results in PEVK region extension (145). Thus, it seems clear that titin contributes to the increased tension seen at long sarcomere lengths, but the mechanisms and consequences of titin's interactions with active elements in contracting skeletal muscle is not known.

In an attempt to determine the primary factors that cause muscle injury, Warren et al. (152) damaged rat soleus muscle *in vitro* and used a multiple regression analysis (factors of peak tension, lengthening velocity, change in length and initial length) to conclude that peak tension is the most important predictor of muscle damage. This result was supported by the findings of McCully and Faulkner (98), who reported that peak force experienced by muscles during lengthening

contractions was strongly correlated with reduced functional capacity three days after injury ($r = -0.70$) and with histological evidence of structural damage ($r = 0.79$). Thus, it is reasonable to conclude that high force correlates with exercise injury, but there is not conclusive evidence that high force alone is the responsible factor.

2.3.2 High Strain as the Initiating Event

In 1988, a study of the effects of lengthening contractions on human elbow flexors at differing muscle lengths found that there is a length-dependant component in the force loss and the development of pain measured 24 hours after exercise (105). This idea was later investigated by Lieber and Friden (87), who designed a unique study to determine whether muscle damage is a function more related to peak force or to active strain. In their first experiment, muscles were stretched either before or at peak tetanic force. This produced identical strains (25% of fiber length) but 25% higher force magnitudes in the late stretched muscles. In contrast to the findings implicating high force as the primary cause of injury (98, 152), the differing forces in the two treatments induced similar levels of damage as measured by loss in P_o one-hour after injury. In a second experiment, Lieber and Friden repeated these conditions only using 12.5% strain. Again, peak force was lower in early-stretched muscles, but the observed decrement in P_o was similar between groups. Thus, muscles subjected to 12.5% strain had less damage than

those experiencing 25% strain, which resulted in the conclusion that active strain, not peak force, was the primary cause of lengthening-contraction injury (87).

This conclusion was supported by the findings of Talbot and Morgan (140) who reported that initial length, active strain, and number of contractions, but not force per se, were strong determinates of the decline in P_o seen in exercise-injured frog sartorius muscles (140). These studies have clearly demonstrated that active strain is an important function related to muscle injury, but the question remains as to what aspect of the active lengthening causes the loss in functional capacity.

It has long been known that passive lengthening that remains within physiological parameters does not cause injury to skeletal muscle (62). Therefore, it is reasonable to conclude that an interaction between active and passive elements might exist. To address this idea, Bruton, et al. (26) investigated the possible existence of a mechano-sensitive link in mechanisms of EC coupling. Single frog skeletal muscle fibers were fatigued before passive stretch (20% of fiber length). Using this preparation, they found a long-lasting reduction in P_o in 6 of 35 of these experiments and concluded that there is an easily damaged mechano-sensitive link involved in EC coupling in fatigued muscle fibers. Thus, evidence that 20% stretch magnitudes do not cause injury in the absence of actively cycling crossbridges suggests complex interactions between passive and active components.

In keeping with this idea, Brooks, et al. (25) performed a series of experiments that tested the hypothesis that the magnitude of injury is a function of both strain and force, e.g. the work done on a muscle. To test this hypothesis, they

measured damage, using loss of force and ultrastructural evidence immediately following single stretches of whole mouse muscles *in situ.* The results from this experiment supported the hypothesis that the work done on a muscle is the best predictor of the magnitude of muscle injury. This has been supported by findings of lengthening-contraction-induced injury to atrophic muscle, where the decline in P_o was most highly correlated with pre-stretch tension (resulting in more work for a given strain) (144).

2.3.3 Sarcomere Length Inhomogeneity as the Initiating Event

Studies supporting the idea that muscle damage is a function of strain or work (strain x force), suggest that it is the increase in muscle length during active contractions that is the key factor in the initiation of injury. Morgan (101) has developed a hypothesis that explains how sarcomeres are susceptible to disruption at longer sarcomere lengths. Morgan's sarcomere-popping hypothesis predicts that inherent sarcomere length inhomogeneities are responsible for the damage seen after repeated lengthening contractions The descending limb of the length-tension relationship reflects diminishing sarcomere force capacity at long sarcomere lengths. According to Morgan's theory, when an active muscle is lengthened, some sarcomeres may move onto the descending limb of their length-tension relation. If neighboring sarcomeres remain at their length-tension plateau, they are by definition stronger than the extended sarcomere. Any additional increase in muscle length will then occur at the expense of the longer, weaker, sarcomere.

As active lengthening continues, the extended sarcomeres are further lengthened, which further reduces their force capacity and ultimately results in sarcomere failure (101). The theoretical result of this failure is the development of over-extended sarcomeres that are randomly distributed throughout the muscle. These sarcomeres are predicted to be extended to the point where the actin and myosin filaments no longer overlap, and tensile stress must be derived entirely from passive structures. Morphological evidence showing randomly distributed hyper-contracted half-sarcomeres adjacent to hyper-extended half-sarcomeres show this to be one consequence of muscle injury and gives strong support to Morgan's theory (106).

In an effort to validate the popping-sarcomere hypothesis, Talbot and Morgan (141) examined toad fibers that had been rapidly fixed after single active stretches without being allowed to shorten. These fibers showed 8.4% of sarcomeres with myofibrils not overlapping in one half of the sarcomere. Fibers that were allowed to relax and shorten after identical contractions showed <1% of sarcomeres with non-overlapping myofibrils (141). This suggests that stretched sarcomeres re-interdigitate during shortening and that multiple lengthening contractions of physiological strain are needed to produce significant structural damage. Other studies find similar results. Brooks, et al. (25), found single active stretches of whole muscles (< 30% strain) produced no force deficit, while studies using multiple-contraction protocols consistently result in significant injury as evidenced by up to 70% decline in P_o (90, 152). Thus, multiple lengthening

contractions appear to result in a reduced ability to reinterdigitate and the overextension and eventual failure of sarcomeres.

If a significant number of these "popped" sarcomeres are in series, one could expect the length-tension relation to shift to longer muscle lengths. This result was first observed by Katz in 1939 (77) and has since been well documented in studies using multiple lengthening contractions (14, 103).

In summary, lengthening contractions cause injury in skeletal muscle. In support of Morgan's hypothesis, evidence suggests that these muscle injuries occur by the overextension of sarcomeres that are on the descending limb of the length-tension relation. Because lengthening contractions would be expected to increase the number of sarcomeres on their descending limb, this type of muscle activity would be more likely to produce sarcomere popping and damage than isometric or shortening contractions.

2.4. Calcium in Exercise-Injured Muscle Cells

A critical consequence of overextended or popped sarcomeres after injury is an uncontrolled rise in intracellular [Ca^{2+}]. This loss of calcium homeostasis is a key event that is postulated to cause a number of degenerative processes in skeletal muscle. These include mitochondrial dysfunction due to calcium overload (7), degradation of myofibrillar, intermediate-filament and membrane-associated proteins (56), and the possible activation of phospholipases leading to degradation of membrane lipids (73).

Numerous cellular mechanisms in skeletal muscle rely on the precise regulation of Ca^{2+}. For example, muscular contraction and relaxation depend upon controlled release and reuptake of Ca^{2+} by the sarcoplasmic reticulum (SR). The importance of this mechanism in skeletal muscle is perhaps well indicated by the presence of at least 7 membranous systems for transporting Ca^{2+} (30), which are responsible for roughly 30% of total cellular energy cost under resting conditions (1). A brief explanation of the physiological mechanisms of calcium signaling and homeostasis in skeletal muscles follows.

During normal resting conditions, intracellular Ca^{2+} is maintained at very low levels (10^{-8}M to 10^{-6}M) primarily by Ca^{2+} adenosine triphosphatase (ATPase) pumps located in the membrane of the SR. The Ca^{2+}ATPase protein functions by pumping Ca^{2+} into the lumen of the SR, where some of the free Ca^{2+} binds to calsequestrin. The presence of calsequestrin in the SR reduces the intraluminal $[Ca^{2+}]$ and consequently the electro-chemical gradient the Ca^{2+}ATPase must pump against. This gradient nonetheless is in the order of 10,000:1 (1). A similar gradient exists between the intra- and extracellular space. It has repeatedly been proposed that exercise injury disrupts these calcium-handling mechanisms, which, by allowing Ca^{2+} to flow down its electrochemical gradient, causes a sustained increase in intracellular $[Ca^{2+}]$ (3, 7, 13, 20). These and other studies (14, 71, 94, 126) have shown that calcium is increased in association with exercise injury.

2.4.1 Ca^{2+} Influx Across the Sarcolema

Extracellular calcium influx across the sarcolema can be observed by incubating muscles in a bath containing Ca^{2+} or ^{45}Ca. Using this technique, Armstrong, et al. found an increase in total muscle calcium associated with both passive and active stretch-induced injury in soleus muscles of the rat (7). A similar result, using mouse muscles, was reported by Lowe et al. (91). Confocal microscopy of a limited number of these fibers showed no increase in intracellular $[Ca^{2+}]$. As a result, it was concluded that cellular buffering maintained Ca^{2+} homeostasis and that elevated $[Ca^{2+}]$ is unlikely to be a critical event in response to muscle injury (91). In contrast to this conclusion, Jones et al. (75) and Gissel et al. (57) found calcium influx across the sarcolema in association with contractile activity in mouse and rat respectively. The mechanism for this calcium influx has not been fully elucidated; however, one possible source is the stretch-activated Ca^{2+} channel located in the sarcolema.

2.4.2. Ca^{2+} Influx through Stretch Activated Channels

The dihydropyridine (DHP) receptor is a membrane-bound calcium channel (31). The primary role of the DHP receptor is its voltage-sensitive signaling, which transmits action-potential impulses from t-tubules to the ryanodine receptor in the membrane of the SR. However, the DHP receptor is also found throughout the sarcolema and is thought to function as a stretch-sensitive calcium channel (31). The function of these DHPs, which are independent of ryanodine receptors, has not

been well described, but their existence is well documented (46). Thus, the DHP receptor may be a mechanism of Ca^{2+} ingress through the sarcolema. Armstrong et al. (7) reported that holding rat soleus muscles in passive stretch resulted in a 62% increase in total muscle calcium. The calcium-channel blocker (CCB) verpamil, blocked these elevations in intracellular calcium (7). Similarly, amlodipine (a long acting CCB) suppressed desmin degradation and indices of ultrastructural damage in human subjects following lengthening contractions of the knee extensors (17). These data suggest that one source of the increase in intracellular calcium after damage may be stretch-activated channels, but it is also possible that the CCBs used in these studies stimulated Ca^{2+} buffering mechanisms such as mitochondrial Ca^{2+} uptake (17). Thus, the available evidence indicates the presence of a stretch-induced mechanism of Ca^{2+} ingress after injury, but the etiology of this process requires further elucidation.

2.4.3 Impaired or Damaged Sarcoplasmic Reticulum

Three possible SR-related mechanisms have been identified that may result in increased intracellular [Ca^{2+}] after exercise injury. First, Ca^{2+} may leak into the intracellular space through ruptures in the SR membrane. This is postulated to occur as a result of the mechanical damage to T-tubules and SR membranes that has been observed after injury. One study found evidence of several types of morphological anomalies in T-tubules and SR membranes after downhill-running exercise in rats (139). T-tubule damage was also seen in single fibers from mouse

flexor digitorum brevis muscles subjected to lengthening contractions (155). These studies clearly show damage to T-tubular and SR membranes, but this does not directly indicate that increased [Ca^{2+}] after injury comes from an intracellular source. To address this question, muscles were incubated in A23187 (a Ca^{2+} ionophore) in Ca^{2+}-free media (116). These muscles showed significant signs of Ca^{2+} injury. Thus, evidence suggests there is sufficient Ca^{2+} within the SR pool to activate autolytic mechanisms and that the increased [Ca^{2+}] seen after exercise is in part due to rupture of SR membranes (116, 139).

Second, there are a number of reports that indicate that Ca^{2+} pumps are inhibited, damaged, or otherwise unable to keep up with the Ca^{2+} load during both non-damaging and damaging contractile activity. High-intensity exercise generates several metabolic byproducts and conditions that are known, or suspected, to inhibit Ca^{2+} pump function. These include super oxide anion, depletion of glycogen, adenosine diphosphate (ADP), H^+, and high temperature (28, 135). Changes in these factors tend to be transient, e.g. are modulated within 60 minutes after cessation of exercise (29), and therefore are defined as fatigue-related mechanisms (45). One possibility is that these transient factors contribute to lasting damage, even though the initiating factor is no longer present. Although there are data that show Ca^{2+} pump function is inhibited in single fibers immediately after stretch (13) and in human quadriceps 30 minutes after cycling to exhaustion (22), it is unknown whether Ca^{2+} pump function is inhibited on a long-term basis after exercise damage.

Finally, Jackson (73) proposed that high post-injury [Ca^{2+}] causes excessive mitochondrial Ca^{2+} accumulation and may result in a local depletion of the supply of ATP to Ca^{2+}ATPase pumps in the SR. This could act as a positive-feedback loop, where dysfunction of Ca^{2+} handling by the SR results in more free-Ca^{2+} in the cell, which contributes to further mitochondrial dysfunction, etc. An early study, using *in vitro* isometric contractions in mouse soleus, found mitochondrial Ca^{2+} was not related to the enzyme efflux associated with contractile activity (73). It is unlikely that this result applies to mechanisms of muscle injury, because the muscles in this study were likely only fatigued. Duan, et al. (38) damaged rat solei in a downhill-walking preparation and found mitochondrial Ca^{2+} uptake was related to muscle injury. Thus, limited data suggest mitochondrial overload may play a role in the etiology of the injury process.

2.4.4 Intracellular [Ca^{2+}] After Injury

Despite the widespread speculation concerning the importance of an increase in [Ca^{2+}] after injury, there are surprisingly few studies that actually show one exists. This is, in part, due to the technical difficulties involved in measuring minute changes in intracellular [Ca^{2+}]. The majority of reported values of intracellular [Ca^{2+}] after injury range between 40 and 250 nM (14, 71, 94), although one study reported a value of 1.02 μM after an ultra-marathon event (111). These values represent relative increases above normal resting [Ca^{2+}] of 50 to 120%. Data from these few studies show that [Ca^{2+}] rises as a consequence of exercise injury in

skeletal muscle and it is this rise in [Ca^{2+}] that is proposed to activate mechanisms of the autogenic phase.

2.5 The Autogenic Phase

The autogenic phase consists of intrinsic processes that occur at the local site of injury (8). These may include the phospholypase-A_2 cascade, the lysosomal proteases and the Ca^{2+}-activated proteases. The loss in function, cellular disorganization and increased protein degradation that occurs following injury may be related to the function of one or more of these mechanisms, which are reviewed in the following sections.

2.5.1 The Phospholypase-A_2 Cascade

Phospholipase-A_2 (PLA_2) is a Ca^{2+} activated membrane-bound enzyme that is associated with the production of arachidonic acid and subsequently directly affects cellular inflammatory response (36). Arachidonic acid may act to degrade proteins associated with the sarcolema (8, 40). However, one study found that inhibition of PLA_2 with various drugs did not prevent or diminish myofilament damage from calcium overload in skinned amphibian skeletal muscle (40). In addition, PLA_2-deficient murine hearts were likewise unprotected from calcium overload after ischemia-reperfusion, suggesting that another mechanism is responsible for injury in these models (36). Combined, these data argue against a

prominent role for PLA_2 in the development of contractile injury in skeletal muscle or myocardium; however, further study is likely warranted.

2.5.2. The Lysosomal Proteases

Lysosomes are small cytoplasmic organelles that contain over 50 hydrolytic enzymes, including several of the cathepsins which are cysteine proteases (53). There are several factors known to regulate lysosomal proteolysis. These include intraluminal redox conditions, pH, and $[Ca^{2+}]$ (for review see ref 113). Inhibition of lysosomes does not reduce total protein breakdown in rat skeletal muscle exposed to starvation (a condition that increases $[Ca^{2+}]$) (93) or A23187 (a Ca^{2+} ionophore) (53). Therefore it appears unlikely, although not shown directly, that lysosomal mechanisms play a key proteolytic role in response to increased $[Ca^{2+}]$ in skeletal muscle.

2.5.3 The Proteosome

The ubiquitin (Ub)-proteosome pathway relies on Ub "tagging" to identify proteins for degradation by the proteosome complex. Ubiquitination requires ATP and occurs in a 3-step process that is catalyzed by E1, E2, and E3 ligases (85). The proteosome complex is a 2.1 MDa multi-subunit proteolytic enzyme that is shaped like a barrel with four stacked rings. The active sites of the proteosome are isolated within the inner surface of the structure, which protects against non-specific digestion of proteins (85). In addition, the small diameter of the inner core of the

proteosome requires that proteins marked for digestion must be unfolded prior to entry. Consequently, the proteosome can degrade actin and myosin only when they have been released from the normal myofilliment lattice (128).

Protein degradation by the proteosome has been implicated in various pathologies, including cachexia (128), renal failure (12), and atrophic conditions caused by space flight (70) and denervation (54). In addition, there are increases in indices of proteosome activity, such as ubiquitin levels, after lengthening-contraction exercise in humans (120, 136) and chronic contractile activity in rabbit skeletal muscle (110). There are no data that show how proteins are singled out for degradation following injury, but it has been proposed that another protease may exist upstream of the proteosome and act to provide it with monomeric myofibrillar proteins as substrates (69). A likely candidate for that protease is calpain.

2.6 The Structure Function and Regulation of Calpain in Cells

There are currently 14 known human calpain genes. Products of at least five of these genes are expressed in adult skeletal muscle. These include the ubiquitous μ- and m-calpains, p94 (the muscle-specific calpain), calpain-4, and -10 (37). Initially differentiated by their micro- (μ) and milli- (m) molar *in vitro* calcium half-maximal activation requirement, the ubiquitous μ- and m-calpains are widely expressed in nearly all eukaryotic cells (60). Calpains comprise 2-5% of sarcomeric proteins and are closely associated with the Z-line region of the sarcomere (58). Their activation by exogenous Ca^{2+} results in degradation or disruption of the Z-

line, which is a common observation seen in exercise-injured muscle (141). The monomeric p94 isoform, a titin N2-line and M-line binding protein, is the major calpain component in skeletal muscle (138). The absence of the p94 gene has recently been discovered to cause Limb Girdle Muscular Dystrophy 2A (132).

2.6.1. The Skeletal Muscle-Specific Calpain (p94)

Levels of p94 mRNA in skeletal muscle are 10-times more prevalent then the combined mRNA of the ubiquitous calpains (130), yet until recently almost nothing was known about the function or regulation of this isoform. This is due, in part, to the enzyme's propensity for autocatalytic degradation. The recent production of an enzymatically-active recombinant protein has resulted in the determination that p94 is highly sensitive to Ca^{2+} activation at submicromolar levels and is stabilized by binding to titin (23). Because titin is a key protein associated with the structural stability of muscle cells, its stretch-induced disruption may prove to be linked to calpain activity after exercise injury.

In exercise-injured human skeletal muscle, p94 mRNA declines immediately, and remains depressed for 24 hours after exercise injury (44). In contrast, m-calpain mRNA levels increase after injury (129). This inverse relationship has led to the idea that the presence of p94 may inhibit m-calpain activity (44). This evidence suggests an inter-relationship between isoforms in which both p94 and m-calpain are in some way affected by each other and by small (nM) changes in intracellular calcium. Although this is an intriguing idea, it has not

been thoroughly investigated. As a result, the remainder of this review will focus on the function and regulation of the ubiquitous calpains.

2.6.2 Structure of the Ubiquitous Calpains

The μ and m-calpains are heterodimeric proteinases containing 80-kDa and 30-kDa subunits (131). The proteolytically-active 80-kDa subunit contains four distinct subdomains with approximately 60% sequence homology between isoforms. The 30-kDa regulatory subunit has two distinct domains and is not different between isoforms (131). Domain II of the large subunit contains the site for proteolytic activity. The function of the small subunit is not well understood, but it is thought to inhibit the proteolytic activity of the large subunit prior to their Ca^{2+}-activated dissociation. In addition, the small subunit may chaperon 80 kDa renaturation and regulate its Ca^{2+} sensitivity (131). These and other factors that affect the regulation of calpain-mediated proteolytic activity have been the focus of considerable scientific enquiry (60).

2.6.3 The Regulation of Calpain-Mediated Proteolytic Activity

Throughout the 1990's it was generally agreed that the ubiquitous calpains were maintained within cells as inactive proenzymes that required Ca^{2+} binding and autolytic cleavage prior to activation (63, 72, 97, 122). This has been shown to be a sequential process, first involving subunit dissociation, followed by autolysis of the large subunit to a 78 kDa active fragment. In 1999, the successful crystallization of

the m-calpain large subunit revealed that autolysis removes an α-helical NH_2 terminus and that the NH_2 terminus does not block the active site of the intact enzyme (60, 68). It seems likely, therefore, that autolysis occurs as part of a mechanism of calpain activation, but autolysis is not theoretically an essential aspect of enzyme activity (74). Thus, the purpose of autolysis is not well described, but *in vitro* studies have shown that autolysis precedes measurable levels of calpain-mediated proteolytic activity and that autolysis is dependant on $[Ca^{2+}]$ (124, 127).

A preponderance of early research concerning the regulation of calpain has been focused on its *in vitro* Ca^{2+} activation (124), yet an unexplained discrepancy exists between the $[Ca^{2+}]$ required to activate calpain *in vitro* and the much lower $[Ca^{2+}]$ found *in vivo* (60). Later research has linked the regulation of calpain in cells to numerous additional factors, which include the localized distribution of Ca^{2+} (53), cellular location of calpains (55), the ratio of autolyzed to unautolyzed enzyme, the quantity of bound substrate and inhibitor (calpastatin) (58), cellular redox conditions (63), phosphorylation status of both calpain and its substrates (60) and other post-translational modifications such as substrate-binding to calmodulin (64) or an activator protein (114).

In the early 1990's, a 40-kDa endogenous protein was found to increase the Ca^{2+} sensitivity of m-calpain in rat skeletal muscle (114) and human erythrocytes (122). This "activator" protein was reported to have no affect on μ-calpain, but in these experiments it lowered the m-calpain $[Ca^{2+}]$ activation requirement to within

physiological levels (20 nM). This protein has not been purified, and its specific affects on the regulatory properties, e.g. Ca^{2+} binding, of the calpains are not known. No other laboratories have successfully duplicated these experiments.

The early observation that phospholipids reduce the [Ca^{2+}] required to initiate *in vitro* autolytic activation led to the hypothesis that the mechanism of calpain activation might involve binding to cellular membranes (72). Several studies into the properties of calpain activation in association with cellular membranes have reported that calpains bind to membrane-associated proteins, not phospholipids, in membrane vesicles (72, 80, 122). The significance of these interactions is not known. It seems unlikely that membrane binding could be a primary mechanism of calpain activation because calpains do not appear to be localized near the membrane (59). In skeletal muscle, the calpains are distributed throughout the interior of the cell, with no preferential localization near the plasma membrane (81). Similarly, in human erythrocytes, less than 7% of the total calpain is associated with the membrane (123), suggesting that if membrane binding is the sole mechanism of activation, either 93% of calpains are inactive or they must translocate to the membrane to be activated. In this regard, there are limited data that support the idea that calpains may translocate within the cell to be activated.

Autolytic activation of μ-calpain has been associated with membrane translocation in human platelets (4) and rat skeletal muscle. Calpain-like activity was increased in membrane fractions of spin-fractionated skeletal muscles of rats after treadmill exercise to exhaustion (9). These data support the idea that

translocation and membrane binding may be one mechanism of calpain regulation. In keeping with this idea, there are consistent data that show calpains bind to membrane proteins (80); however, conflicting results have been reported concerning the affects of this binding on their autolytic activation. In 1989, Inomata (72) speculated that calpain binding to membrane-associated α-fodrin induced autolysis and release of activated calpain into the cytoplasmic milieu. This result was not supported by the findings of Goll, et al. (59), who found no increase in autolytic activation of calpain under similar conditions. There are currently no well-described mechanisms that would explain how or why the calpains would migrate to the membrane in order to be activated. Thus, it seems reasonable to speculate that calpains are activated, at least partially, by a mechanism other than membrane binding. So, the mechanisms of activation and regulation of the calpains in living cells remain largely unexplained.

2.6.4. Functions of Calpain

Although calpains have been the subject of intense scientific interest, questions remain concerning their functional purpose under normal and pathological conditions. In addition to their proteolytic role, calpains are involved in activation/regulation of enzymes, cleavage of hormone receptors, chemotactic stimulation of inflammatory mechanisms, and apoptosis (for a complete review see (60). Calpains do not entirely degrade proteins into their amino acid components, but rather cleave proteins in a limited site-specific manner. As a result, their

postulated role in muscle cells is to initiate disassembly of damaged sarcomeres fated for degradation by other mechanisms, possibly the proteosome (69, 76). This could provide a mechanism to explain the morphological alterations such as Z-line streaming seen in exercise-injured muscle and is corroborated by evidence of calpain cleavage of a large number of structural muscle proteins.

2.6.5. Substrates of the Ubiquitous Calpains

Numerous proteins have been identified as *in vitro* substrates of calpain. In skeletal muscle these include the Z-line and membrane-associated proteins desmin, vinculin (69) vimentin (104), fodrin and α-sarcoglycan (44), and the myofibrillar proteins, tropomyosin, C-protein, troponin-I and troponin-T and titin (see pg. 138 of ref 151 for complete list).

Titin is a 3 mDa protein approximately one micron in length. Its putative function is to support passive tension and myofibrillar alignment and re-interdigitation after stretch (150). The gradual re-interdigitation failure that occurs after repeated lengthening contractions could be related to damage to the titin molecule (102). In addition, the degradation of titin is thought to contribute to morphological alterations such as the wide A-bands seen in exercise-damaged tissue (89, 144). At long sarcomere lengths the molecule may "pop" off the thick filament at the C-terminal end of the protein, which is also the general location of a bound p94 molecule (150, 151). It is not known whether this type of overextension of the sarcomere has an effect on the activation of p94.

Fodrin, also called αII-spectrin, is a ubiquitous 280 kDa membrane-associated protein that plays a role in the maintenance of cell shape and cell integrity, the generation and/or maintenance of cell polarity, and the formation of cell adhesion complexes (142). In skeletal muscle, α-fodrin is located in the costamere, and has been shown to interact with the costameric proteins ankyrin, plectin, desmin and muscle LIM-protein (42).

Although these and nearly 100 other proteins have been identified as *in vitro* substrates of calpain, there are no data that suggest an *in vitro* substrate of calpain is also cleaved *in vivo* (60). Limited evidence suggests substrate phosphorylation (58) or binding to calmodulin (64) may affect substrate susceptibility to calpain degradation; however, no single characteristic that predisposes a protein as an *in vivo* calpain substrate has been identified. In spite of this, there are considerable data that implicate calpains with the structural alterations that are seen after exercise injury in skeletal muscle.

Calpains in skeletal muscle are primarily located at the Z-disk (59). Accordingly, *in vitro* activation of calpain in muscle cells releases α-actinin from the Z-disk (presumably by digestion of zeelin-1 and zeelin-2) and causes disruption or dissolution of the Z-line (27). Similarly, a common observation in exercise-damaged tissue is disruption of the regular appearance of Z-lines (39, 47, 52, 61, 144). Thus, the disruption of the Z-disk, which occurs in both of these models, supports the idea that calpains are activated after lengthening-contraction injury. These data have been generated, in part, by experiments using exogenous Ca^{2+}

overload in skeletal and cardiac models of muscle injury which are reviewed below.

2.6.6. Ca^{2+} Overload in Skeletal and Cardiac Cells

Calpain can be experimentally activated in cells by manipulating intracellular [Ca^{2+}]. *In vitro* experiments, using Ca^{2+} ionophores (a channel that allows Ca^{2+} influx from the interstitium or efflux from the SR) in both amphibian and mammalian muscle fibers, have shown that steady-state [Ca^{2+}] in the nM range can rapidly elicit damage that is similar to exercise-induced injury (39). Using this type of preparation, Duncan (39) observed 11 types of ultrastructural damage associated with increased [Ca^{2+}]. These observations were found to be both time- and [Ca^{2+}]-dependent and were categorized into those that disrupt the organization of the myofilaments without the appearance of contraction, and those that affect the Z-line and may have a hyper-contracted appearance (39). This damage occurred at [Ca^{2+}] within physiological levels. One possibility is that prolonged elevation in [Ca^{2+}] at this concentration activated calpains. A second possibility is that the skinned fibers used in this study did not contain the endogenous inhibitors to proteolytic enzymes that are present in living fibers. Thus, these models provide valuable information concerning unregulated Ca^{2+}-activated proteolytic activity in cells, but the physiological relevance of these observations is unknown.

Models that are likely more physiologically relevant include exogenous Ca^{2+} overload or ischemia followed by reperfusion, in cardiomyocytes or intact

hearts. It has been well documented that Ca^{2+} handling is compromised during ischemia and reperfusion in cardiac cells (96, 148). These conditions induce an immediate loss of contractile function, which is accompanied by the degradation and release of the myofilament proteins α-actinin, troponin-I, and myosin light chain-1 (96, 148), and the intermediate filament proteins desmin and spectrin (118). When calcium chelators (EDTA or EGTA) or the cysteine protease inhibitors leupeptin or E64, are present, protein breakdown is suppressed, suggesting that calpains are the mechanism by which these proteins are degraded (118). In addition, exogenous Ca^{2+} overload-induced contractile dysfunction in rat hearts has been linked to the degradation of α-fodrin by calpain (146).

These data suggest that calpains are involved in the biological response to injury in cardiac cells. A key event that links the mechanisms of injury in these models with the injury that occurs in exercise-injured skeletal muscle is an increase in $[Ca^{2+}]$. Thus, the proteolysis that occurs in each model may be mediated by the same mechanism: the Ca^{2+}-induced activation of calpain.

2.6.7 The Role of Calpains as Mediators of the Autogenic Phase

The idea that calpains are activated in skeletal muscles after strenuous exercise was initially investigated by Belcastro. In 1993, Belcastro (18) published a seminal article detailing the results of a series of experiments that examined calpain activity in the homogenates of rat hind-limb muscles after exhausting horizontal treadmill exercise (18). Calpain that was purified from these muscles was found to be more sensitive to Ca^{2+} activation (e.g. the force pCa^{2+} curve was shifted to the left) and showed an increase in total caseinolytic activity under saturating Ca^{2+} conditions. In addition, an increased susceptibility to calpain degradation was observed for the myofibrillar proteins α-actinin, tropomyosin, desmin and vimentin in muscles from exercise-exhausted animals (18).

These and several other observations support the hypothesis that calpains are activated after injury. First, there is a growing body of evidence that show sustained damage-associated increases in intracellular $[Ca^{2+}]$ (7, 9, 13, 17) and there are now limited data indicating that calpains are activated *in vivo* by $[Ca^{2+}]$ at these levels (112). Second, the Ca^{2+}-induced force loss in mechanically skinned fibers of rat and toad is both pH- and temperature-dependent, which suggests the involvement of an enzymatic mechanism (83). Third, there are considerable data that suggest several key structural proteins that are *in vitro* calpain substrates (see section 2.6.5.) are also degraded after injury (49, 139, 141). The 12-hour post-injury delay in peak damage to desmin (15) supports the idea that an enzymatic proteolytic mechanism is involved. Fourth, the use of calpain inhibitors has been

shown to attenuate both the decline in P_o after Ca^{2+} induced cardiac injury and the associated increase in proteolysis that is seen in these models (118, 146).

None of these findings can be considered conclusive. First, reports of a sustained increase in $[Ca^{2+}]$ sufficient to activate calpains are few. Thus, the disruption of Ca^{2+} homeostasis after damage seems likely but has not been proven. Second, the loss in force that occurs immediately after injury has been shown to be, in part, dependent on temperature, but this loss in force in one study was not attenuated by calpain inhibitors (154). These researchers concluded another enzymatic mechanism, other than calpain, was responsible for the loss in force (154). Third, the structural alterations and subsequent force losses that are seen after lengthening-contraction injury or Ca^{2+} overload have not been directly linked to the proteolysis of individual proteins. Thus, the similarity between these observations in exercise-injured and calpain-activated models cannot be considered conclusive evidence of calpain activity after injury.

Thus, a majority of evidence suggests, but does not prove, that mechanical damage to Ca^{2+}-handling structures causes a loss of Ca^{2+} homeostasis that results in the activation of calpain in exercise-injured skeletal muscle. This idea was presented in 1991 by Armstrong et al. (8), and was formulated into a more formal hypothesis seven years later by Belcastro et al. (19). The hypothesis was again put forward by Gissel and Clausen 2001 (56); however, little direct evidence has been generated to support this theory.

2.6.8. Evidence that Calpains are Activated after Muscle Damage

Belcastro's 1993 experiments showed that several aspects of calpain-mediated proteolysis are altered after exhaustive horizontal treadmill exercise. Nonetheless, there are a number of questions that were not answered by these experiments. First, it has been well established that there are many factors that affect calpain activity *in vivo* (see section 2.6.3). Because Belcastro's assays were performed *in vitro*, his conclusions may not apply to the dynamic conditions within living cells. Second, in Belcastro's study, the increased susceptibility of myofibrillar proteins to calpain-mediated degradation occurred with saturating levels of Ca^{2+}, which clearly does not represent physiological conditions. Third, a distinction between the effects of fatigue and muscle damage is not possible using an exhaustive running model. Thus, it remains equivocal whether calpains are activated *in vivo* after exercise, whether myofibrillar protein susceptibility to degradation by calpain is increased at the $[Ca^{2+}]$ found in injured cells, and whether calpain activation is unique to damaging exercise or is a generalized response to prolonged contractile activity.

2.7 Summary and Hypothesis

A majority of evidence suggests that mechanical mechanisms are responsible for the disruptions in cellular structure that are seen after exercise injury in skeletal muscle. Although still under investigation, it appears that these structural alterations cause a loss in Ca^{2+} homeostasis, leading to an increase in

intracellular [Ca^{2+}]. It has been widely postulated that this increase in intracellular [Ca^{2+}] activates the calpains, which cleave a number of key proteins and may initiate a feed-forward cycle leading to increased susceptibility to damage (8, 19, 20, 117, 133, 157). Calpain activation would serve to link disruptions in calcium homeostasis to increased proteolysis and may act as the key event in the initiation of the autogenic phase of protein degradation following an exercise event.

While there are considerable data that support this idea, it has never been directly tested. The purpose of this project was to directly test this idea by investigating the following hypothesis.

2.7.1 Hypothesis

We hypothesize that *in vivo* calpain-mediated proteolysis will increase in rat skeletal muscles injured by lengthening contractions but not in muscles subjected to non-damaging contractions. To test this hypothesis we will:

1. Develop an apparatus to induce *in situ* lengthening contraction injury in extensor digitorum longus (EDL) muscles of anesthetized rats.
2. Evaluate *in vivo* calpain-mediated proteolytic activity in damaged skeletal muscles by quantifying the breakdown of α-fodrin, a highly specific and sensitive marker of calpain activity (69, 146).

CHAPTER 3

A New Apparatus for Studying Exercise Injury in Skeletal Muscle

Kevin Marley and Jeffrey J. Widrick

Department of Exercise and Sport Science

3.1. Abstract

Skeletal muscles subjected to repetitive active-lengthening contractions undergo substantially more damage than muscles subjected to isometric or shortening contractions. Thus, the study of exercise-induced injury to the skeletal muscles under controlled conditions requires an apparatus capable of lengthening active muscles. Traditional devices used to perform this task utilize torque motors that require considerable financial resources to acquire and relatively complex software to run. We developed a simple apparatus, using inexpensive and readily available materials, that is capable of inducing lengthening contractions in hindlimb muscles of anesthetized laboratory animals (in this case, rats). The device consists of a force transducer affixed to a linear actuator. The actuator is driven by a stepper motor that is controlled by simple command language via a desktop computer's serial port. Custom programming coordinates muscle stimulation, actuator displacement and force data acquisition. The device can produce reliable (± 0.03 mm) high resolution (3.15 um) changes in linear displacement while recording the subsequent force response of the muscle under study.

3.2. Introduction

It has been well established that lengthening contractions (also termed eccentric, or pliometric contractions) cause injury to skeletal muscles (5, 90). These injuries are associated with symptoms of pain, swelling, and reduced range of motion. These symptoms increase over the 24-48 hours after injury, but then subside and are resolved over the next 5-14 days (126). Despite considerable scientific inquiry, an understanding of the mechanisms of contraction-induced injury and recovery remains incomplete.

A number of models have been developed to study these mechanisms under controlled conditions (38, 120, 158). These include: 1) voluntary exercise such as those that involve treadmill running (18), or resisted joint extension (119); 2) electrically stimulated contractions in intact anesthetized animals (43); 3) *in vitro* preparations that use single muscle fibers (102) or whole muscles (52) and 4) *in situ* preparations that isolate and stimulate particular muscles within their physiological environment.

Running models offer advantages for studying generalized responses to exercise, but one disadvantage is that no distinction can be made between responses that result from non-injurious contractile activity or contractile activity that causes muscle damage. Electrically stimulated intact animal preparations have the advantage of a high degree of physiological relevance, but these models lack the ability to adequately control or monitor the magnitude of the stress or strain experienced by individual muscles. Preparations that activate whole muscles or

single fibers *in vitro* trade off these disadvantages for controllability but do so at the expense of physiological relevance and may subsequently have external validity problems.

Perhaps the model that provides the most experimental control, while maintaining a high degree of physiological relevance, is the *in situ* preparation. These preparations produce accurate measurements of stress and strain experienced by the muscles under study. An additional benefit is the ability to perform experiments without disrupting blood flow or other systems of cellular homeostasis.

In situ preparations require a method of controlling muscle length and measuring muscle force during stimulation. Torque motors, capable of simultaneously measuring muscle force while altering muscle length, are typically used to accomplish this. Several elegantly designed systems have used torque motors as effective tools for inducing injury in skeletal muscles *in situ* (21) and for observing subsequent changes in their contractile properties (10). However, torque motors and the associated electronics required for their control are expensive. The financial resources required to obtain these devices may not be available to all researchers.

Clearly an inexpensive and readily available apparatus for the study of exercise-induced injury in skeletal muscle would be of great benefit. In this paper we describe a relatively inexpensive and easily constructed apparatus that provides

the capability to precisely control *in situ* muscle length in active rodent hindlimb muscles.

3.3. Materials and Methods

3.3.1. Apparatus

The key mechanical component of this system is a linear actuator used to manipulate muscle length (Figure 3.1). The actuator converted the rotary motion of a motor-driven ball-screw into linear movement. A carriage, with internal threads, moved forward or backward along two rails in response to rotation of the ball-screw.

The ball-screw was driven by a 5-volt, DC stepper-motor (VEXTA, C6831-9292, Scituate, MA). Each pulse delivered to the motor rotated the ball-screw by 1.8°. The pitch of the ball-screw was such that each pulse delivered to the motor produced a 3.15μm linear displacement of the carriage.

An isometric force transducer (Harvard Apparatus, model 60-2996, Holliston, MA) was securely mounted on the carriage of the actuator. The entire stepper motor, actuator, and transducer combination was attached to a sturdy base. Also mounted to the base was a rigid, adjustable frame constructed using standard laboratory 1.27 cm aluminum rod and nylon connectors. This frame, supported a 1.91 cm thick Plexiglas platform, upon which the experimental animal was secured. The stepper motor and frame were arranged so that the animal's hindlimbs

extended towards the actuator/transducer and were aligned with the actuator's movement.

3.3.2. Instrumentation and Control

A desktop computer and a data-acquisition board (E-series, National Instruments, Austin, TX) were used to control muscle stimulation and actuator displacement while simultaneously collecting data from the force transducer. Muscle stimulation was accomplished by a Model 701A Aurora Scientific High-Power Bi-Phase Stimulator (Aurora Scientific Inc., Aurora, Ontario, Canada). The stimulator operated in response to text file commands delivered from one of the analog output channels of the data-acquisition board as described below.

Actuator displacement was controlled by a stepper-motor controller card (Pontech STP100, Rancho Cucamonga, CA) that had been interfaced to the computer through a serial-port. String communication motor-control commands, consisting of a one- to five-digit code for pulse-interval (displacement speed), displacement direction, and total number of pulses (displacement amplitude) were used to program the board as described below. The commands necessary to produce a specific displacement were determined empirically.

Transducer output was sampled (10 kHz) by one of the analog input channels of the data-acquisition board.

3.3.3. Programming

The data-acquisition board was controlled by a custom program written using LabView graphical programming language (version 6.1, National Instruments, Austin, TX). A schematic outline of the program is illustrated in Figure 3.2. After initialization of the input and output channels, the program read the contents of a text file into the analog output buffer. This text file mimicked the desired muscle-stimulation pattern (i.e. stimulus duration, train frequency, train duration) for the particular experiment. The program then entered a For Loop. On each loop iteration, the data-acquisition board sent the stimulation pattern to the muscle stimulator (operating in its "follow" mode), output control commands to the motor-controller board that initiated actuator movement at the appropriate time, and stored output from the force transducer in a buffer. The contents of this buffer were written to a text file upon the completion of each loop iteration. The total number of loop iterations, and the duration of the delay between each loop iteration, were specified by the user. The program also had the capability of recalling force files for analysis.

3.3.4. *In situ* Preparation

All experimental procedures were approved by the Oregon State University Institutional Animal Care and Use Committee. Rats were anesthetized using isoflurane (2-3%) delivered in 100% O_2. Depth of anesthesia was monitored so that

respiratory rate was 50-60 breaths/min and the animal had no response to a toe pinch.

The tendon of the left EDL was exposed above the retinaculum, and a small loop (silk suture, 2-0) was tied to the tendon. The tendon was then severed and a drop of cyanoacrylate glue was applied to the suture to keep the suture from pulling off during contractions. The peroneal nerve was exposed at the distal lateral aspect of the knee and a bi-polar electrode (Harvard AH 50-1650) was placed around the nerve and connected to the muscle stimulator. The electrode was stabilized by closing the skin at the incision site with cyanoacrylate glue.

The animal was placed in a supine position on the Plexiglas platform. The foot was stabilized with Velcro and tape and the knee was secured with a clamp. A 21-gauge stainless-steel rod with hooks at both ends was used to connect the suture loop on the EDL tendon to the force transducer. A heating pad attached to the under-surface of the platform, and a radiant heat lamp suspended above the platform, were used to maintain muscle temperature at 35-36°C (monitored by a needle thermocouple inserted into the contralateral triceps surea). Alignment of the longitudinal axis of the EDL with the actuator's plane of motion was accomplished by raising or lowering the Plexiglas platform. Fore-aft alignment was accomplished by sliding the platform back and forth. Once the muscle had been aligned, the platform was secured to the frame of the apparatus using C-clamps.

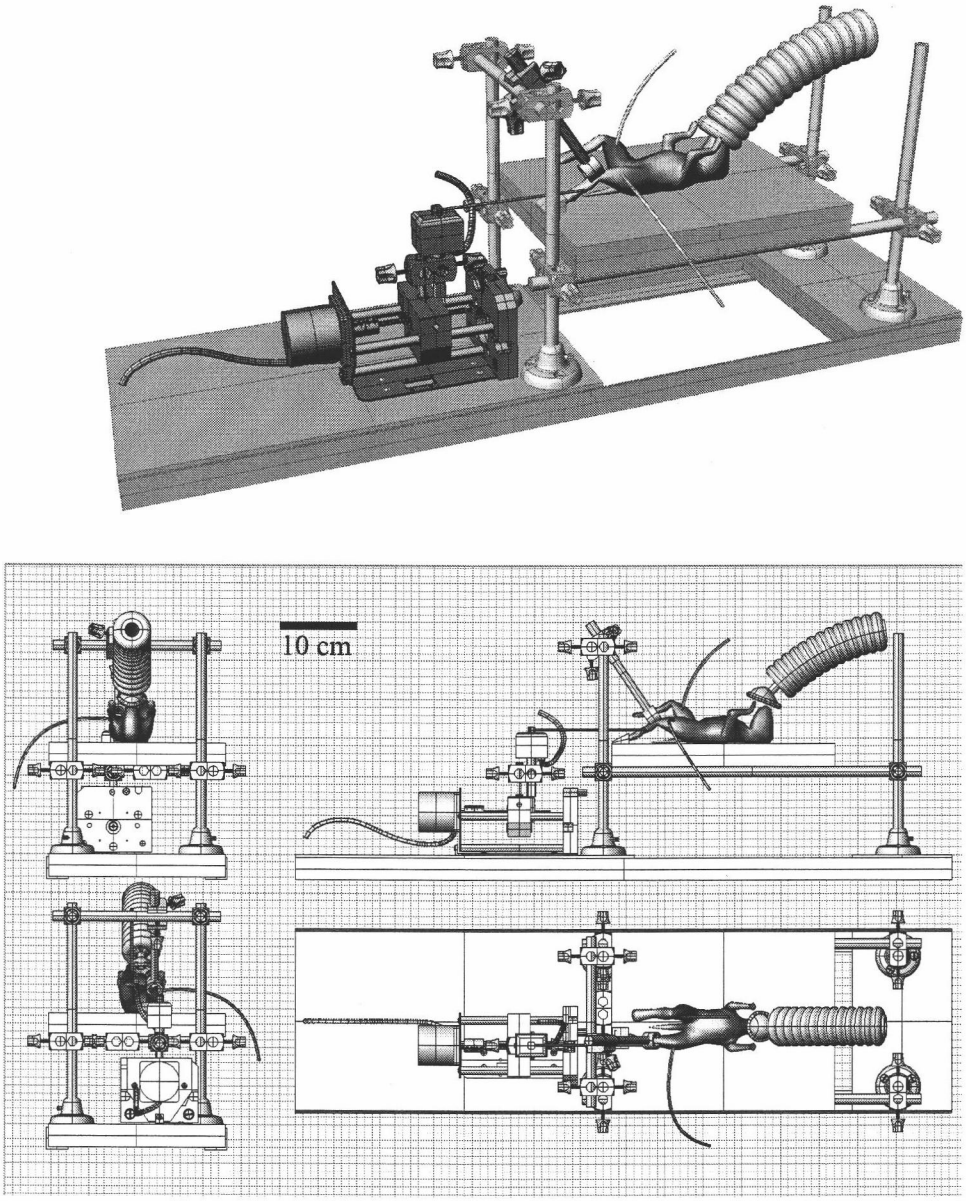

Figure 3.1. Computer rendered image of apparatus in perspective (top), and end, side and top view (bottom). The animal is placed on a plastic platform. The adjustable frame supporting the platform is made from nylon connectors (#21708, VanWaters and Rogers, Goshen, PA) and standard 1.27 cm aluminum rod. The plastic platform was secured to the frame with C-clamps during experiments (not shown). The linear actuator was purchased complete in the form shown. The force transducer was affixed to the top of the moveable carriage with a bolt and nylon connector.

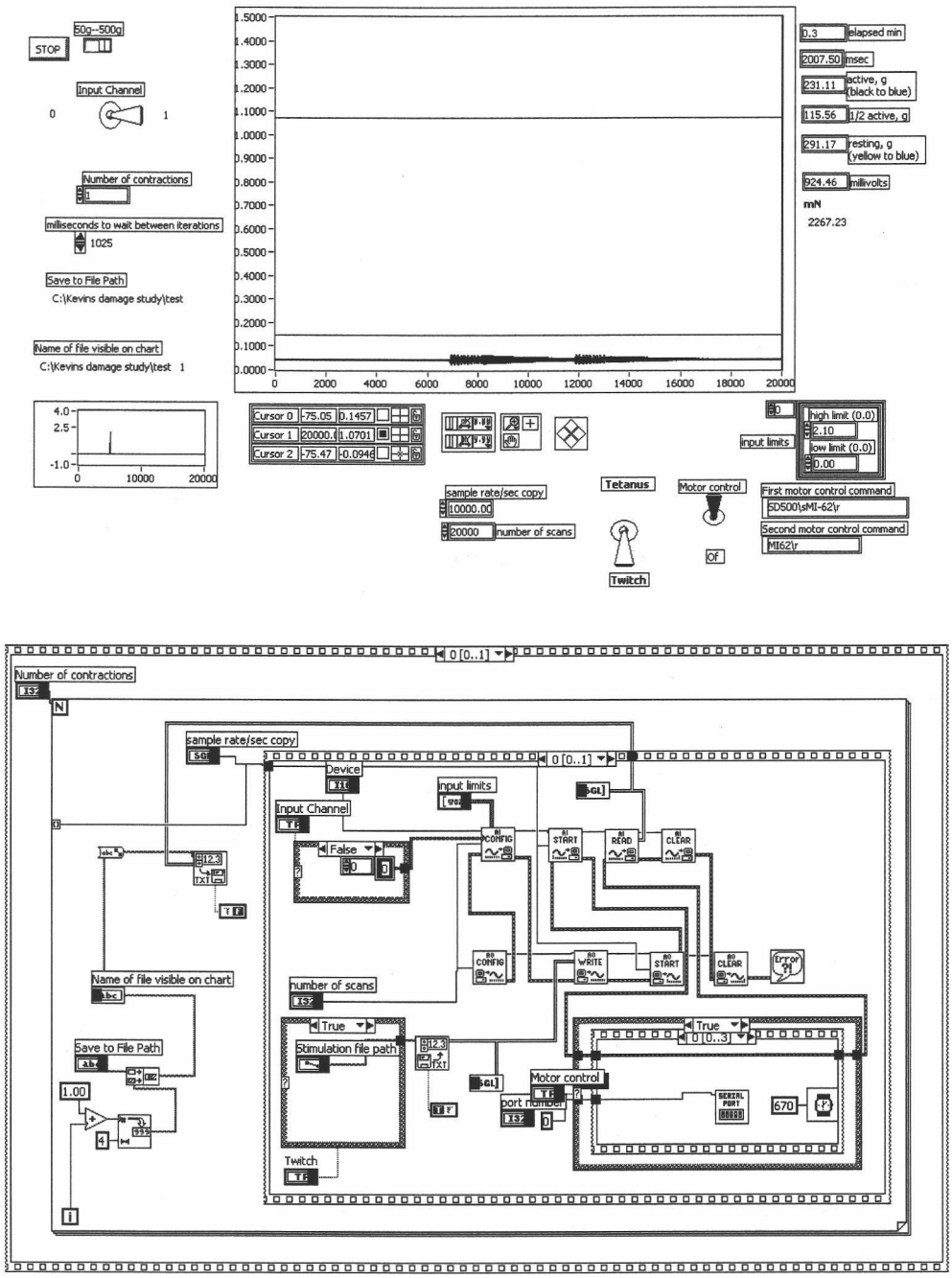

Figure 3.2. Front and back panels of LabView software that controls linear actuator, muscle stimulator and data collection.

3.3.5. Reliability and Resolution Measures

A calipers capable of measuring 0.05 mm was used to assess the repeatability of the linear actuator movement by measuring a programmed displacement of 2 mm at a movement speed of 12.5 mm/sec. This was repeated ten times and compared against an equal number of measurements of a fixed distance of 2 mm. In addition, the measurement error of the calipers was tested by measuring a fixed object 10 times.

Resolution capability was assessed by measuring the displacement of the carriage that resulted from a 100-pulse movement command. This distance was then divided by 100 to determine the displacement/pulse.

Accuracy of movement speed was assessed using an oscilloscope (Hewlett Packard, #54645A, Palo Alto, CA) to measure elapsed time of unloaded force-transducer movement. These measurements were made in triplicate at 12.5, 18.75, and 25 mm/sec velocities.

3.3.6 Muscle Stimulation and Stretch Parameters

Optimal muscle length was determined as the muscle length where the force response to a 500 μs square pulse was maximized. Fine adjustments in muscle length were accomplished by manual rotation of the ball-screw. Tetanic contractions were obtained at optimal length (L_o) using supramaximal stimulation at 200 Hz (Figure 3.3). For the lengthening contractions shown in Figure 3.4, the muscle was allowed to come to peak isometric force during the initial 100 ms of

stimulation prior to lengthening at three different velocities. Assuming a L_f/L_o ratio of 0.44 (25), and a muscle length of 30 mm, a displacement of 2 mm in this muscle approximates a 15% L_f strain. The lengthening contractions, therefore, consisted of a 2 mm displacement applied over 160, 116, and 81 ms to represent 1.0, 1.5, and 2.0 fiber lengths/sec respectively. After the stimulation ceased, the muscle was given approximately 350 ms to relax to its new resting force baseline and then returned to its original L_o at the same speed at which it was lengthened. At the end of the experiment, the tendon of the tibialis anterior was severed and the muscle retracted. The L_o of the EDL was measured with calipers before being excised from the animal and weighed. The animal was killed by exsanguination. The cross-sectional area (CSA) was calculated according to the following formula;

$$\text{CSA } (mm^2) = \frac{\text{muscle mass (mg)}}{L_f \text{ (mm)} \times 1.06 \text{ (mg/mm}^3\text{)}}$$

where L_f is 0.44 times muscle length and 1.06 is muscle density (10).

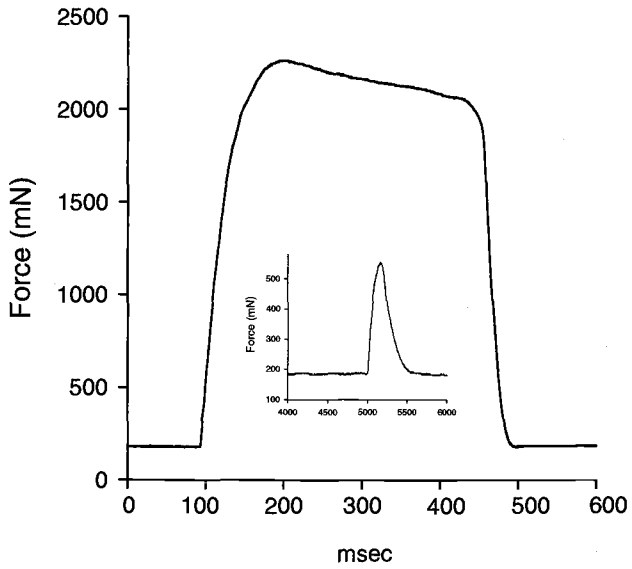

Figure 3.3. Representative isometric twitch (inset) and tetanic force traces from a *in situ* rat extensor digitorum longus muscle (mass = 0.149 g; L_o = 30.00 mm) Peak twitch force was 370 mN. Peak tetanic force was 2082 mN, which corresponds to a specific force of 195.5 kN/m^2. Supra-maximal stimuli through the peroneal nerve consisted of a 0.5 msec square wave stimulus, and a 360 msec 200 Hz train of stimuli for the twitch and tetanus, respectively. Maximal tetanic force occurred within 100 msec of initial stimulus.

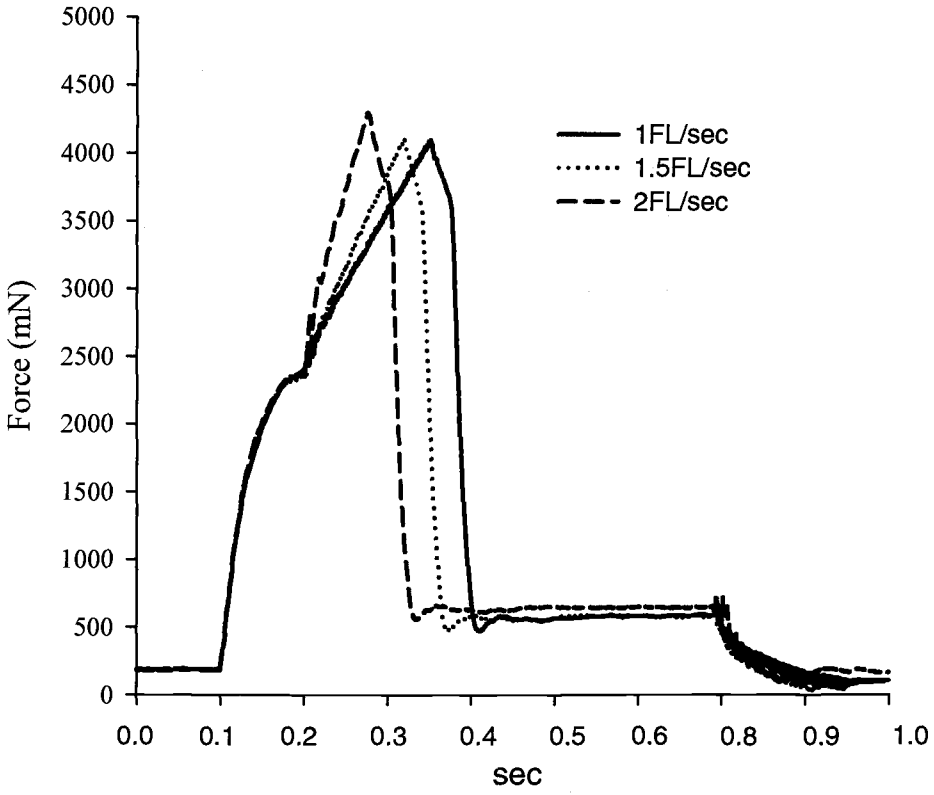

Figure 3.4. Force traces of lengthening contractions at three speeds (indicated in legend). The muscle was allowed to come to peak isometric force for 100 ms prior to lengthening. Displacement was 2 mm for all contractions, which approximates 15% of fiber length (see text). Peak lengthening contraction force was 3904, 3920, and 4104 mN at 1.0, 1.5, and 2.0 FL/sec lengthening velocities respectively. Stimulation and displacement for each contraction speed were timed to cease simultaneously, whereupon the force fell to that produced by passive structures. After 800 ms, muscle length was returned to L_0.

3.4. Results and Discussion

The resolution capability of this system was 3.15 um/step, which is likely adequately precise for most applications. The mean displacement as measured for 10, 2 mm movements was 1.98 ± 0.03 mm. The reliability of the carriage movement was equal to that of the calipers in our hands (Table 3.1). Unloaded movement velocities were highly reproducible, so that mean time to travel 2 mm varied by less than 0.04 sec for the three speeds tested (data not shown).

Fixed Distance (mm)	Measured Displacement (mm)
2.00	1.95
1.95	2.00
2.00	2.00
2.00	2.00
1.95	2.00
2.00	2.00
1.95	1.95
2.00	1.95
2.00	2.00
2.00	2.00
Sum 19.85	19.85

Table 3.1. Caliper values for ten consecutive measurements of a fixed 2 mm distance (left column) and after ten programmed displacements of 2 mm (right column). The summed values are identical. Thus, the repeatability of the programmed movements was equal to or better than the measurement error of the calipers.

The apparatus was easy and inexpensive to construct using readily available materials and provided consistent, reproducible results in a variety of configurations. We designed our device to adapt an existing system capable of

studying isometric contractions to a system providing lengthening-contraction capability. As such, only the actuator and control card, plus small miscellaneous hardware, were required beyond our existing equipment. The linear actuator was purchased used for $50 on an online auction and the motor control card was purchased separately from the manufacturer for $150. Thus, our total cost was less than $250 (2003 prices). Obviously, the cost will be higher for those laboratories that do not presently have the capabilities of studying isometric contractions. In this case the minimum additional equipment required would include a desktop computer, AD board, software, muscle stimulator and isometric force-transducer.

The linear actuator in this system is capable of movement speeds up to 25 mm/sec. A more sophisticated actuator would be capable of higher speed. However, it should be noted that rapid accelerations may not be possible with this design due to potential noise problems associated with acceleration of the large mass of the force transducer. In addition, the large distance from the top of the force transducer to the supporting rails of the actuator in the current configuration resulted in some system compliance. This compliance was effectively eliminated by the resting tension that was placed on the system. However, it would likely be advantageous to mount the force transducer closer to the center of the carriage, especially if smaller muscles with lower resting tension (i.e. mouse muscles) are to be studied.

The LabView software is a user-friendly icon-based format that can easily be adapted to perform a variety of functions by persons without extensive training

in computer programming. The device has already been used to successfully study lengthening-contraction injury in EDL muscles of rats, but there are a wide range of possible applications. These could include different muscles or species depending on how the device is configured and the capacity of the force transducer that is used.

CHAPTER 4

Calpain-mediated proteolytic activity in exercise-injured skeletal muscle

Kevin Marley[1], Neil E. Forsberg[2], and Jeffrey J. Widrick[1]

[1] Department of Exercise and Sport Science and [2] Department of Animal Sciences

4.1. Abstract

Skeletal-muscle damage induced by lengthening ("eccentric" or "pliometric") contractions results in an immediate loss in maximal tetanic force capacity (P_o), and an increase in protein degradation by unidentified endogenous mechanisms. We hypothesized that increased proteolysis following active lengthening injury is caused by the Ca^{2+}-dependent protease calpain. We tested this hypothesis by measuring the calpain-specific proteolysis of α-fodrin in rat extensor digitorum longus (EDL) muscles subjected to either 90 *in-situ* active lengthening contractions (17.4 ± 0.3% of fiber length), 90 active isometric contractions, 90 passive extensions (18.4 ± 0.1% of fiber length) or no contractile treatment. Sixty minutes after the exercise treatments, isometric force declined 4 ± 2% of P_o in the isometric contraction treated muscles (n = 6), 4 ±1% in passive lengthening muscles (n = 3), and 5 ±3% in no contractile treatment muscles (n = 3). In contrast, force declined 53 ± 3% of P_o ($P < 0.01$, vs. all groups) in muscles subjected to lengthening contractions (n = 6). Calpain-mediated fodrinolysis produces 145 kDa and 150 kDa peptides that retain immunoreactivity to the intact α-fodrin antibody. Analysis of Western blots showed that levels of these peptides were not different for the three non-injury treatments. In contrast, levels of the 145 kDa and 150 kDa peptides were significantly elevated ($P < 0.01$) in muscles subjected to lengthening contractions. These data indicate that calpain-mediated proteolysis is increased in rat EDL muscle injured by *in situ* lengthening contractions.

4.2. Introduction

The biological responses to the injuries that occur when muscles repeatedly resist their own lengthening have important implications to the understanding of sport and occupational injuries and to the etiology of diseases that involve muscle dysfunction. It has been long recognized that these so-called lengthening, eccentric, or pliometric contractions are associated with sarcomere disruption (47), muscle-protein efflux into the systemic circulation (129), muscle dysfunction (153), and delayed-onset muscle soreness (126).

In the past decade, much attention has focused on the mechanisms that initiate damage during lengthening contractions. This work has been summarized in several recent reviews (2, 34, 115). The rapid loss of key structural proteins (79, 89) and increases in muscle-protein degradation (92) following injury are proposed to result from the activation of localized intrinsic processes, termed autogenic mechanisms, that are activated immediately after injury (5, 14, 89). Little is known about how these autogenic responses are regulated in damaged skeletal muscle.

One characteristic of exercise-induced muscle damage is a rise in intracellular Ca^{2+} concentration ($[Ca^{2+}]$) (3). Consequently it has been proposed that the Ca^{2+} regulated cysteine protease calpain may participate in the autogenic response to injury (19). In support of this hypothesis, Belcastro (18) reported increased calpain activity, increased sensitivity to Ca^{2+} activation, and increased myofibrillar substrate susceptibility to calpain degradation in hind limb muscles obtained from rats subjected to exhaustive level treadmill exercise. Calpain activity

has also been reported to increase nearly two-fold after chronic stimulation in rat skeletal muscle (137).

These data suggest that calpain activity increases after both acute and chronic exercise. However, the *in vitro* assays used in these studies measured calpain activity after exposure to a maximal concentration of activating Ca^{2+}. It seems unlikely that this represents the $[Ca^{2+}]$ in the intracellular environment of the cell under *in vivo* conditions. Furthermore, the *in vivo* activation of calpain involves many factors, such as interactions with its endogenous inhibitor calpastatin (60), intracellular redox state (63), cellular location (membrane proximity) (122), temperature, pH, and phosphorylation status (143). Thus, it is unclear how calpain activities measured *in vitro* correspond to the activity of the enzyme under the prevailing *in vivo* conditions of the exercise-injured muscle cell. Finally, it is not clear whether changes in calpain activity previously reported are a characteristic of muscle injury per se or simply a generalized response to exhaustive contractile activity.

The purpose of this study was to assess the *in vivo* activity of calpain following active lengthening-induced muscle injury. We hypothesized that calpain-mediated proteolysis would be elevated in muscles recovering from lengthening-induced injury but not in muscles recovering from non-damaging contractile activity. To test this hypothesis we evaluated the *in vivo* degradation of α-fodrin (or αII-spectrin), a well characterized marker of calpain mediated proteolysis (69, 121, 146), in rat extensor digitorum longus muscles injured by lengthening contractions.

4.3. Methods

4.3.1 Animals

Male Sprague Dawley rats (Simonson Laboratories, average mass (± SE) 312 ± 4.5 g, 3-4 months of age) were used in this study. All experimental procedures were approved by the Oregon State University Institutional Animal Care and Use Committee.

4.3.2. In situ Preparation

Animals were anesthetized with ~2.5% isoflurane in 100% O_2 delivered at 500 cc/min. Depth of anesthesia was controlled by adjusting the concentration of isoflurane to maintain an absence of reflexive pain response and a respiratory rate of 50-60/min. A small incision was made in the skin above the distal tendon of the left extensor digitorum longus (EDL). The EDL tendon was exposed by blunt dissection at and slightly above the retinaculum. A small silk suture (2-0) loop was securely tied to the tendon. A drop of cyanoacrylate glue was applied to the suture to prevent slippage due to the high forces attained during the experimental trials (i.e. the lengthening contractions). Exposed tissue at the incision site was kept moist throughout the experiment with warm saline (0.9% NaCl). To access the peroneal nerve, an incision was made through the skin and first layer of muscle tissue at the distal lateral aspect of the knee. A bi-polar electrode (AH 50-1650, Harvard Apparatus, Holliston, MA) was placed around the nerve and connected to a muscle stimulator (Model 701A, Aurora Scientific, Ontario, Canada). The skin at

the incision site was closed around the electrode with cyanoacrylate glue in order to stabilize the electrode and prevent tissue desiccation.

A device was constructed to subject the EDL to a controlled and reproducible lengthening protocol (Figure 4.1). The apparatus consisted of an isometric force transducer (model 60-2996, Harvard Apparatus) mounted on the carriage of a linear actuator. The actuator was driven by a 5V, DC stepper-motor (VEXTA, C6831-9292, Scituate, MA, 1.8°/step). Programming written in our laboratory (LabView version 6.1, National Instruments, Austin, TX) controlled a data-acquisition board (E-series, National Instruments) that was used to sample the output of the force transducer (10,000 Hz), coordinate muscle stimulation, and control actuator displacement via a stepper-motor controller board (Pontech STP100, Rancho Cucamonga, CA).

The animal was placed supine on an adjustable Plexiglass platform (Figure 4.1). The ankle was positioned in plantar flexion by securing the foot to a small wedge-shaped block using Velcro straps and adhesive tape. The tibia was aligned with the plane of movement of the actuator by adjusting the height of the platform and its fore and aft position. Once aligned, the platform was clamped securely in place. To prevent movement of the lower limb during muscle stimulation, the knee was immobilized in a clamp that was secured to the frame of the apparatus. The EDL tendon was severed distal to the suture loop. One end of a 21-gauge stainless-steel rod was hooked through the loop of suture and the other end hooked around the input post of the force transducer. Intra-muscular temperature was monitored by

inserting a thermocouple directly into the contralateral gastrocnemious. The temperature of this muscle was maintained at 36° C with a heating pad affixed under the platform and a heat lamp placed above the animal.

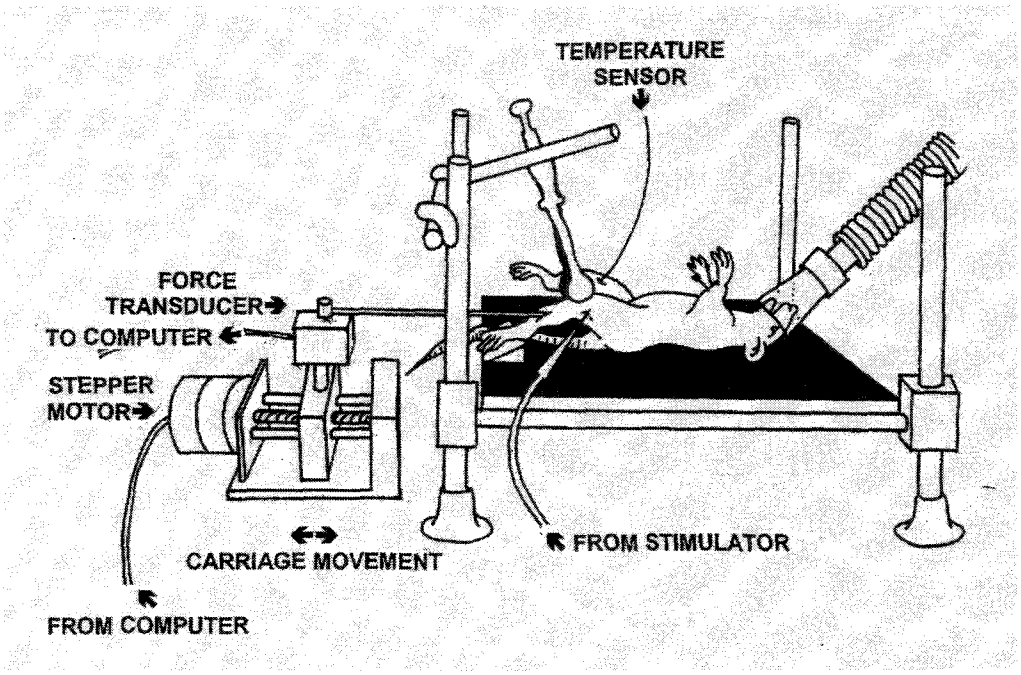

Figure 4.1. Perspective view of apparatus (not to scale). The left foot was affixed to the apparatus with a combination of Velcro and tape (not shown).

The length of the EDL could be manipulated by manually rotating the ball screw of the actuator. Muscle length was adjusted to attain the peak isometric twitch force response to a supramaximal, 500 μs square-wave pulse. This muscle length (L_o), stimulus duration, and stimulus current were used for all subsequent tetanic contractions. To reduce the effects of muscle fatigue, we chose the shortest

possible contraction time that would allow muscles to achieve maximal isometric tetanic force (P_o) prior to lengthening. Pilot data indicated that 200 Hz effectively tetanized the muscles in this preparation and that peak tension was obtained within the initial 200 ms of stimulation. Thus, in order to allow for a 133 ms period of lengthening following P_o (see below), a 333 ms stimulus train at 200 Hz was used for all tetanic contractions.

4.3.3. Experimental Treatments

After the initial setup, tetani were produced every 5 min during a 15 min equilibration period (4 contractions total). This equilibration period was used to ensure that the preparation was stable before initiation of the treatment protocols. P_o rose slightly between the 1st and 2nd contractions and then remained stable, varying by less than 5% between the 3rd and 4th contractions. The average of the last 2 equilibration tetani was therefore taken as the pre-P_o value used in statistical analysis.

Animals were randomly assigned to one of four experimental treatments. These treatments included two active trials, consisting of lengthening contractions (N = 6 animals) or isometric contractions (N = 6), and two trials consisting of passive lengthening (N = 3) or no contractile treatment (N = 3). The general procedure common to all experimental treatments was as follows: three 2-min treatment periods, each separated by a 16 min recovery period, with the final recovery period extended to one hr (98 min for the entire experiment).

Lengthening contraction treatment. Normal physiological strains in the EDL are no greater than 30-35% of fiber length (L_f) (10). Pilot data indicated that a displacement of 2 mm in the rat EDL would approximate a 20% L_f strain, assuming a L_f/L_o ratio of 0.44 (25). The lengthening-contraction treatments, therefore, consisted of a constant velocity 2 mm displacement applied over 133 ms (Figure 4.3. "A"). Thus, muscles undergoing lengthening contractions were allowed to come to peak isometric force during the initial 200 ms of stimulation. The muscle was then lengthened 2 mm during the remaining 133 ms of stimulation. The stimulation ceased and the muscle was allowed 370 ms to relax to its new resting force baseline before being allowed to shorten 2 mm (in 133 ms) back to its original L_o (see Figure 4.2 for sample force traces from both lengthening- and isometric-contraction treatments).

Contractions were administered every 4 sec during each treatment period (30 lengthening contractions per treatment period). For analysis, isometric force was defined as the peak force obtained during the initial 200 ms of stimulation, i.e. peak force prior to initiation of lengthening.

Isometric-contraction treatment. The isometric-contraction trials were identical to the lengthening-contraction treatments, except that the muscles performed fixed-end contractions during the treatment periods (30 isometric contractions per treatment bout). In all cases, peak isometric force was obtained during the initial 200 ms of contraction, allowing valid force comparisons of peak isometric force between the isometric and lengthening treatments.

Control treatments. Each of the previous treatments had a corresponding passive treatment. The lengthening-control trial was identical to the active lengthening-contraction trial except that the muscle was not stimulated during the treatment period. These muscles, therefore, experienced passive lengthening of 2 mm displacement during the treatment periods. Likewise, the non-active-treatment trials were identical to the isometric-contraction trials except that no stimulation occurred during the three treatment periods.

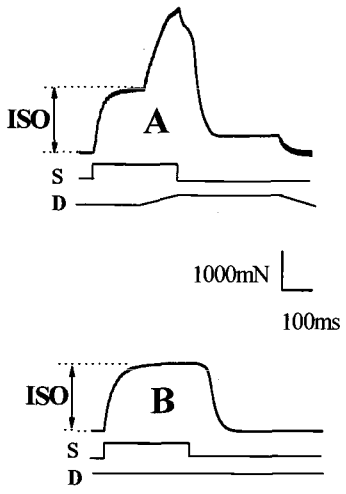

Figure 4.2. Representative force traces from, A) lengthening-contraction treatments, and B) isometric-contraction treatments. A 200 Hz supramaximal stimulus was applied for 330 ms/contraction. Lines designated by S indicate timing of stimulus applied to muscle through the peroneal nerve. Lines designated by D indicate initiation of changes in muscle length (upward displacement indicates an increase in muscle length). Muscles subjected to lengthening-contraction treatments were allowed to come to peak isometric force (ISO) for 200 ms prior to lengthening.

4.3.4. Evaluation of Muscle Recovery

Muscles from all four experimental treatments underwent similar evaluation of force during the three recovery periods. Peak force in response to a fixed-end 200 Hz, 333 ms train was measured at min 0, 5, 10 and 15 min of each recovery period, with additional measurements made at min 30 and 60 of the final recovery period.

4.3.5. Tissue dissection

At the conclusion of the experiment, the tendon of the left tibialis anterior was severed and the muscle retracted. The L_o of the EDL was measured with calipers. The EDL was then rapidly excised from the animal, trimmed of tendon, blotted, weighed, and immediately immersed and stored in liquid nitrogen. Next, the contralateral EDL was dissected, processed, and stored in the same manner. These contralateral muscles served as untreated controls for the Western-blot analysis. Animals were killed by exsanguination.

4.3.6. Tissue Processing and Western Blotting

Muscles were pulverized under liquid nitrogen and suspended in ice-cold Tris-HCl buffer (20mM Tris-HCl, 5mM EDTA, 5mM EGTA, 1mM DTT, pH 7.4) containing a broad-spectrum protease inhibitor cocktail (Roche, #1836170). The protein homogenate was centrifuged (10,000g, 4°C) for ten minutes and the resultant supernatant assayed for total protein concentration using a commercially

supplied kit (Sigma-Aldrich, St Louis, #610A). The solubilized protein was diluted to a concentration of 2.5 mg/ml in loading buffer (62.5 mM Tris, pH 6.8, 2% SDS, 10% glycerol, 5% beta-mercapto-ethanol, 0.001% bromophenol blue), denatured at 100° C for 1min, and electrophoresed in triplicate (25, 37.5, 50 μg protein/lane) on 7% poly-acrylamide gels (7% acrylamide (2.7% bis), 0.375M Tris (pH 8.8) 0.1% SDS, 0.03% APS, 0.1% TEMED). To reduce inter-animal and inter-blot variability, the experimental and the contralateral non-treated control samples from the same animal were always run on the same gel.

Proteins were wet-transferred (25mM tris, 192mM glycine, pH 8.3), overnight onto PVDF membranes (90mA constant current) and blocked with 5% nonfat dry milk in Tween-Tris buffered saline (TTBS, 50mM tris-HCl, 150mM NaCl, 0.05% tween-20, pH 7.4). Blots were probed with mouse anti-spectrin monoclonal antibody (Chemicon, Temecula, CA. #MAB1622) in TTBS (1:1000) for 3-5 hr at room temp. Antigens were detected on x-ray film using the Immun-Star HRP chemiluminescent kit (BioRad, Hercules, CA. #170-5040).

After immunoblotting, films were scanned using the VersaDoc and Quantity One image analysis system (BioRad). Linearity of the signal was confirmed on each blot. The amounts of the proteins in each band were quantified by the intensity of signal after background subtraction. Signal intensity was expressed as arbitrary units (optical density). For each animal, the adjusted volume value ((optical density x area)-background) from blots from the contralateral control muscle (the right EDL) were divided into the value obtained from the

treated muscle (the left EDL). This ratio represents differences in calpain-mediated α-fodrinolysis between muscles. A ratio greater than one indicates more breakdown in the treated muscle.

4.3.7. Electron Microscopy

Muscles used for electron microscopy were treated in the same manner as described above except that upon excision from the animal, the muscles were pinned out at L_o on a Sylgaar base in a petri dish and fixed for a minimum of two hours in Sorenson's phosphate buffer (0.125M, NaH_2PO_4) containing 2% gluteraldehyde (#18420, Ted Pella Inc. Redding, CA.). Fixed tissues were stained in osmium tetroxide prior to dehydration through a graded series of ethanol solutions and imbedding in Spurs resin. The fibers were sectioned longitudinally to approximately 80 nm thicknesses. The sections were supported on Formvar© coated copper grids (Ladd Research, Williston, VT) and stained in uranyl-acetate and lead citrate (35) prior to viewing on a Philips Cm12 transmission electron microscope (FEI Company, Hillsboro, OR.). Images were recorded on film.

4.3.8 Calculation of Muscle Cross Sectional Area

The cross-sectional area (CSA) was calculated according to the following formula;

$$CSA\ (mm^2) = \frac{\text{muscle mass (mg)}}{L_f\ (mm)\ X\ 1.06\ (mg/mm^3)}$$

where L_f is 0.44 times muscle length and 1.06 is muscle density (10).

4.3.9. Statistical Analysis

All statistical analyses were performed using SPSS (version 9.0, Chicago, IL) software. Treatment group differences in muscle mass, L_o, pre- and post-treatment, maximal isometric force at the final recovery-period time point, and fodrinolysis ratios between groups were evaluated by one-way ANOVA. Repeated measures ANOVA was used to compare isometric force, expressed as a percent of pre-treatment P_o, between groups at the 14 recovery time-points. When appropriate, Tukey's multiple comparison tests were used to analyze group differences at indicated time points. One-sample t-tests were used to evaluate fodrinolysis ratios to ascertain if values from treated muscles were different from their corresponding contralateral control muscle. Statistical significance (α) was set at $P < 0.05$. Data are presented as mean ± SE.

4.4. Results

There were no differences in treatment EDL muscle mass (138 ± 10 mg), optimal muscle length (2.86 ± 0.03 cm), pre-treatment maximal isometric force (2.17 ± 0.08 N) or force per cross-sectional area (202 ± 7 kN/m^2) between the four experimental groups. Fiber-length strain for the active- and passive-lengthening groups was 17.4 ± 0.3% and 18.4 ± 0.1% respectively. Although the magnitude of strain between groups was not statistically different, the apparent difference occurred because all animals, regardless of size, were subjected to the same absolute muscle displacement (2 mm).

4.4.1. Electron Microscopy

Electron micrographs from representative muscles subjected to isometric contractions (Figure 4.3A) and no treatment (Figure 4.3C) show a typical orderly arrangement of sarcomere structure. In contrast, the representative micrograph from the muscles subjected to lengthening contractions (Figure 4.3B) has several signs of disorganized or degraded structures. These include disrupted, wavy and miss aligned Z-lines as well as hyper-extended, sarcomeres adjacent to hyper-contracted sarcomeres (a result predicted by Morgan's popping sarcomere hypothesis). Sixty minutes after treatment, the isometric-contraction-treated muscle had completely regained its force capacity, whereas maximal tetanic force produced by the active lengthening-contraction-treated muscle was only 54% of P_o.

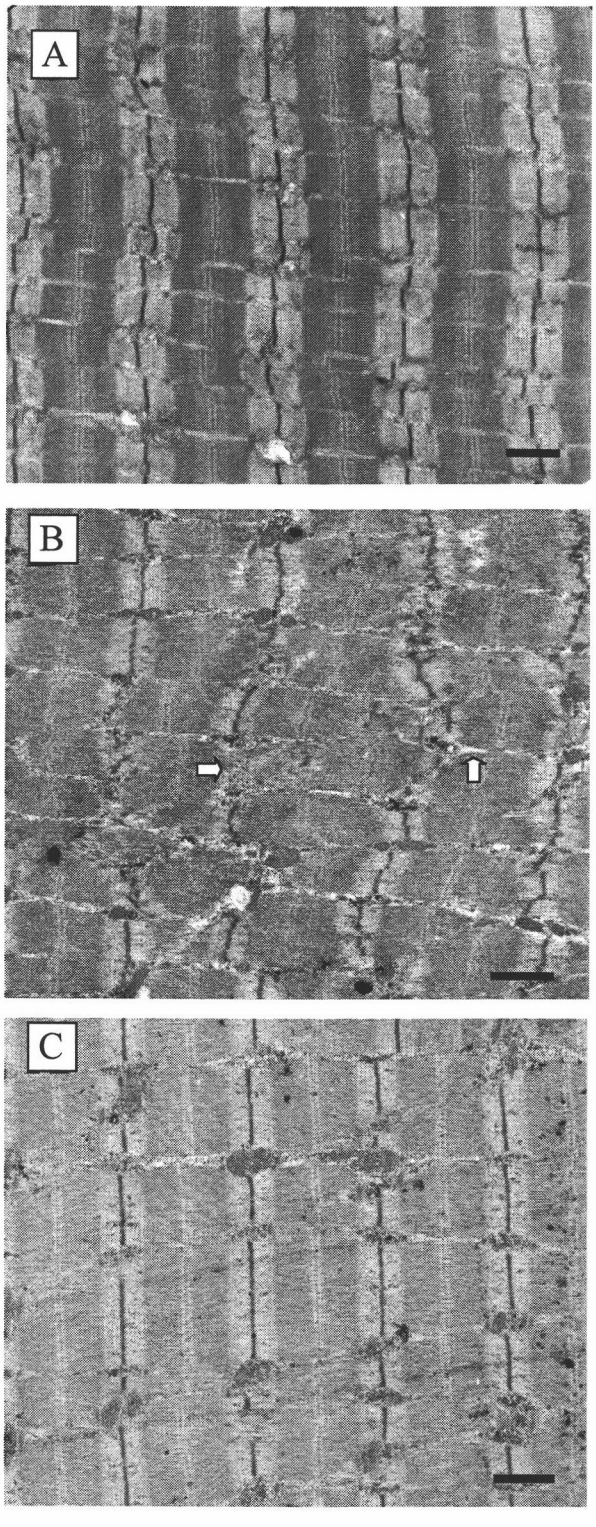
A
B
C

Figure 4.3. Longitudinal electron micrographs of EDL muscles subjected to, A) 90 isometric contractions, B) 90 active-lengthening contractions, and C) no contractile treatment (the muscles shown in B and C were contralateral muscles from the same animal). Force declined 46% of P_o in the muscle subjected to active-lengthening contractions, but was unchanged in the isometric-contraction-treated muscle. The normal striated pattern can be seen in the micrographs from the isometric-contraction-treated and non-treated muscles but sarcomere disruption is clearly evident in the lengthening-contracted-treated muscle. Horizontal and vertical block arrows indicate dissolved and hypercontracted adjacent to hyperextended sarcomeres respectively. Wavy Z-lines can be seen throughout micrograph B. Bars indicate 1 micron.

4.4.2. Force Measurements

Active lengthening treatment. The lengthening contractions caused significant reductions in force during the treatment bouts (Figure 4.4). During bout 1, average force on the 10^{th}, 20^{th}, and 30^{th} contractions declined to 87 ± 6%, 73 ± 6% and 64 ± 7%, of P_o, respectively. There was a 9 ± 4% restoration of force during the first 5-min of the initial 15-min recovery period. However, there was no further increase across the rest of the recovery period.

During treatment bout-2, force was 59 ± 3%, 52 ± 5% and 43 ± 3% of P_o on the 10^{th}, 20^{th} and 30^{th} contractions, respectively. Force recovered 12 ± 4% over the initial 5 min of the second recovery period, but there was no further restoration of force over the remaining minutes of bout-2. The final bout of 30 lengthening contractions caused a further decline, so that isometric force on the 10^{th}, 20^{th}, and 30^{th} contractions was 49 ± 4%, 40 ± 3%, and 33 ± 2% of P_o, respectively.

Force recovered 10 ± 3 % of P_o within the first 5 min of the 3rd recovery period but regained only 4 % more over the remaining 55 min, to result in a lasting force deficit of 53 ± 3%. Thus, muscles subjected to active-lengthening contractions failed to recover tetanic force after cessation of treatment.

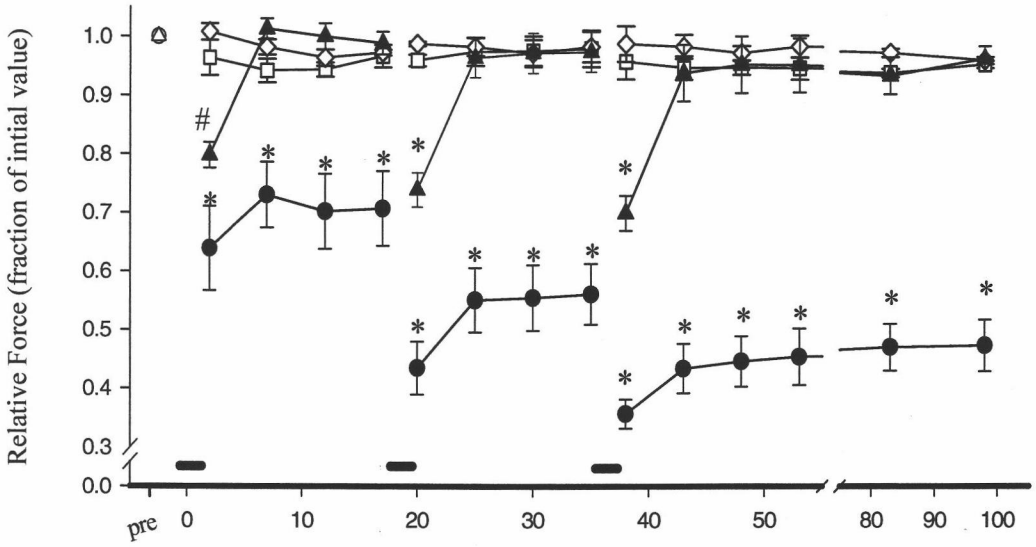

Figure 4.4. Mean isometric force (± SE) from each of the 3 recovery periods for isometric-contraction-treated muscles (triangles), lengthening-contraction-treated muscles (circles) passive-lengthening muscles (squares), and non-treated muscles (diamonds). Horizontal bars indicate time-course of experimental treatments. Note the nearly complete recovery, within 5 min, in the isometric treatment group compared to the active-lengthening contraction group. * Different from all other groups, $P < 0.05$. # Different from control groups, $P < 0.05$.

Isometric treatment. Tetanic force also declined during the isometric bouts (Figure 4.4). By the 10th, 20th and 30th contraction of the isometric treatments, force declined to 90 ± 1%, 84 ± 2% and 80 ± 2% of P_o, respectively. However, in contrast to the lengthening treatment, the isometric-contraction-treated muscles completely regained force capacity within the initial 5 min of each recovery period.

By the end of the experiment, force had returned to 96 ± 2% of initial force, which was not significantly different from the pre-treatment value ($P > 0.05$).

Control treatments. Muscles that underwent passive lengthening or no treatment during the activity bouts displayed little reduction in force during the subsequent test bouts, as force was 95 ± 3% and 96 ± 1% of pre values at the conclusion of the experiment (Figure 4.4).

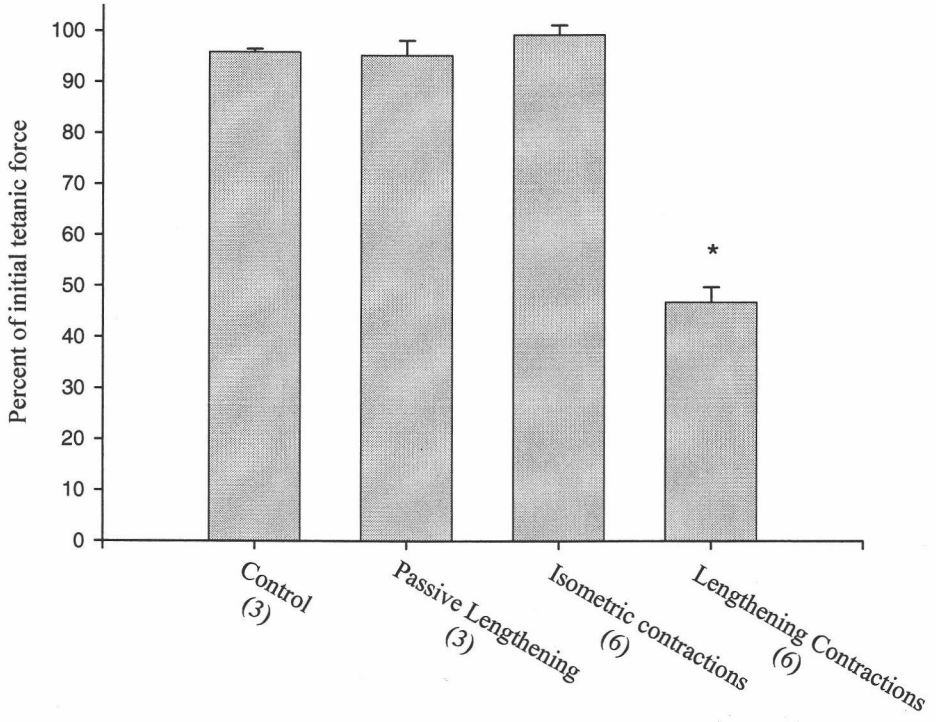

Figure 4.5. Mean tetanic forces from individual treatment groups at the end of experiments (60 minutes after final treatment). * Different from all other groups, $P < 0.01$. Number of animals per group indicated in parenthesis.

One-way ANOVA and Tukey's post-hoc multiple-comparison test indicated a significant difference ($P < 0.001$) between the lengthening-contraction group and

each of the other groups (isometric, lengthening only and control) at the final time-point (Figure 4.5).

4.4.3. Fodrinolysis

For each animal, a ratio of the combined 145kDa and 150kDa signal from treated muscles versus the signal obtained in the untreated contralateral muscles, was determined and used to evaluate the degree of fodrinolysis in the treatment tissues (Figure 4.7). The strength of this approach is that inter-animal and inter-blot variability is controlled. Thus, a ratio value of 1.00 is indicative of equality of fodrinolysis between treatment and contralateral muscles, while a ratio >1.00 indicates greater fodrinolysis in the muscle that received the experimental treatment.

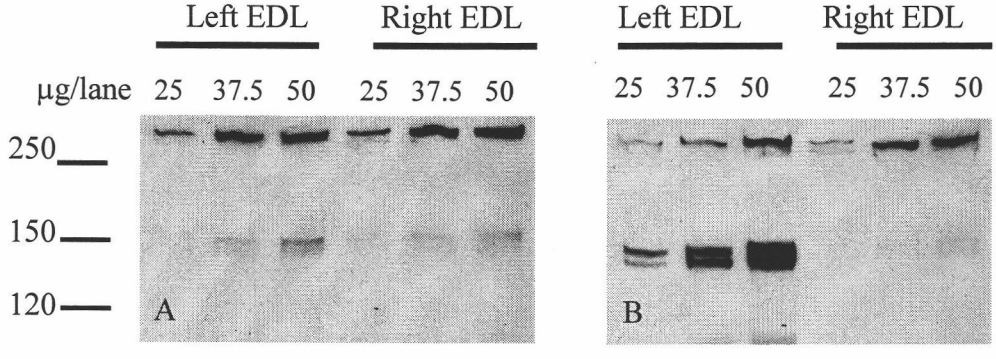

Figure 4.6. Representative Western blots of α-fodrin in EDL muscle homogenates from, A) isometric-contraction-treated, and B) lengthening-contraction-treated animals. The top bands represent intact α-fodrin. The lower bands represent byproducts of the degradation of α-fodrin by calpain. For all animals, the right muscle acted as an internal control. Numbers above lanes indicate amount of protein loaded. Note the large increase in the 145/150kDa signal from the muscle subjected to lengthening contractions.

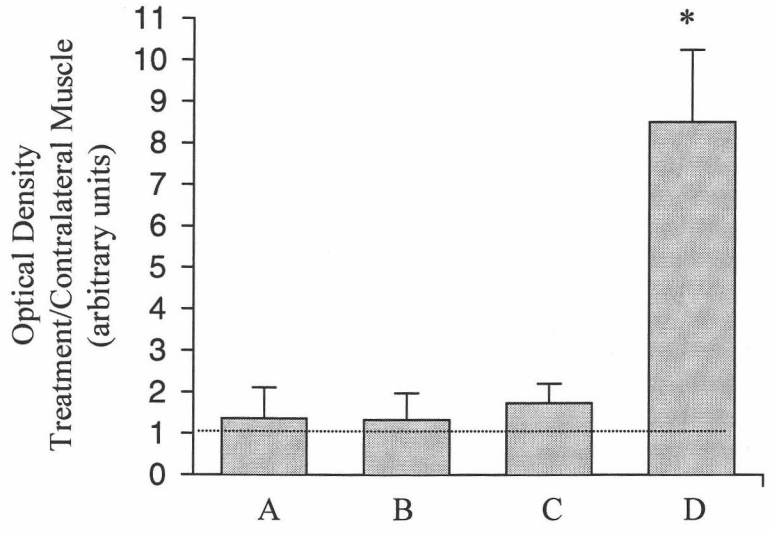

Figure 4.7: Histogram of densitometric analysis of α-fodrinolysis after muscle activity. Bar values are mean ratios (± SE) of the combined 145-150 kDa α-fodrin breakdown products from the left (treated) and right (contralateral) muscles. A) passive, no-treatment, B) passive-lengthening-treatment, C) active-isometric-treatment, and D) active-lengthening-treatment groups. A ratio value of 1 (dotted line), indicates equal α-fodrin breakdown occurred in left and right muscles. Values greater than 1 indicate more α-fodrinolysis in the treatment muscle. * Different from all other groups ($P < 0.01$).

The mean ratio of fodrinolysis breakdown products in treatment to contralateral control muscles was slightly elevated in the passive-lengthening-treated (1.35 ± 0.76), and no treatment contraction (1.35 ± 0.78) groups (Figure 4.8). We assume that this represents a small increase in α-fodrin breakdown as a result of surgery, the recovery test contractions, and tissue processing. Muscles subjected to the isometric-contraction treatment tended to show slightly greater ratios (1.73 ± 0.05), indicating more fodrinolysis. Thus, an additional 90 fatiguing isometric contractions may have resulted in some additional hydrolysis of α-fodrin; however, this difference was not statistically different from either of the two

control trials (ANOVA) or from equality with its contralateral muscle (one-sample t-test).

The ratio of 145 and 150 kDa products in treated and contralateral EDL samples was 8.49 ± 1.74 for muscles subjected to the lengthening-contraction trials. This ratio was significantly greater than the ratio observed for all other treatments ($P < 0.01$). Thus, there was significantly greater fodrin breakdown 1 hr after damaging lengthening contractions compared to all other experimental treatments.

4.5. Discussion

Calpains are a family of endogenous calcium-activated neutral cysteine proteases present in all eukaryotic cells (60). At least 5 of the 14 known human calpain genes are expressed in skeletal muscle. These include the ubiquitous μ- and m-calpains, which are expressed in approximately equal proportions, and the tissue-specific p94 isoform, which is the major calpain constituent in skeletal muscle (60). The μ- and m-calpains are heterodimeric proteases, containing an active 80 kDa fragment (large subunit) and a smaller (30 kDa) regulatory subunit. The p94 isoform, a titin N2-line and M-line binding protein, as well as the other tissue-specific calpains, are monomeric (132, 138).

Because calpains do not degrade proteins into their amino acid components, their proteolytic role in striated muscle likely is to initiate disassembly of damaged sarcomeres fated for degradation by other mechanisms (69, 76). *In vitro* calpain substrates include the membrane-associated and soluble enzymes phospholipase-C,

protein kinase-A, and protein kinase-C; the regulatory proteins tropomyosin, troponin-I, troponin-T; the ryanodine receptor; and the Z-line and costamere associated proteins α-actinin, vimentin, vinculin, α-sarcoglycan, and desmin (44, 58).

An additional target of the calpains is the costamere-associated protein α-fodrin (64, 142). Cleavage of α-fodrin by calpain results in 145 kDa and 150 kDa peptides that retain similar immunoreactivity to the intact protein. Consequently, levels of these immunopositive peptides are a well-accepted marker of calpain-mediated proteolytic activity in striated muscle (69, 146, 157). While the caspases may also degrade α-fodrin, caspase-associated fodrinolysis also produces 120 kDa immunoreactive peptides (78). In this study there were no 120 kDa immunoreactive peptides detected; thus, the appearance of the 145 and 150 kDa signals was attributed to calpain-mediated α-fodrinolysis.

The novel finding of this study is that fodrinolysis increased in exercise-injured muscles but not in muscles subjected to non-damaging contractile activity. Because we utilized an *in situ* muscle preparation and physiological strain magnitudes, it can be concluded that the observed changes in fodrinolysis occurred under physiologically relevant conditions. This represents a major difference between the present results and previous studies in which calpain activity was assessed under *in vitro* conditions that are unlikely to replicate the intracellular milieu of the damaged muscle cells. Therefore, the key conclusion of this study is

that calpain-mediated proteolysis occurred *in vivo* after contractile activity that induced muscle damage, but not after non-damaging treatments.

There are a number of potential mechanisms that could explain our observations of increased calpain-mediated fodrinolysis in muscles damaged by lengthening contractions. First, a loss of Ca^{2+} homeostasis and consequent increase in intracellular [Ca^{2+}] may have led to the Ca^{2+}-induced autolytic activation of calpain. Lengthening contractions similar to those used in the present study have been shown to lead to a disruption in Ca^{2+} homeostasis and a rise in intracellular free calcium ranging from 40 to 250 nM (14, 71, 94). The problem with this idea is that these Ca^{2+} levels are below the 800-15,000 nM [Ca^{2+}] required for half-maximal activation of calpain *in vitro* (60). Despite considerable scientific inquiry, there remains a discrepancy between the [Ca^{2+}] required for *in vitro* calpain activation and that found in cells. One possible explanation for this discrepancy might involve the partial but prolonged activation of calpain at levels that are difficult to detect in *in vitro* experiments. Although this "paradox" remains unexplained, there are limited data that show calpains are active in living cells at physiological [Ca^{2+}].

Recent observations have shown that calpain is active in isolated cardiomyocytes at 451 nM Ca^{2+}, which is near levels reported after injury (97). Additionally, the p94 isoform, which is 10 times more abundant in skeletal muscle than the ubiquitous isoforms, may be regulated by [Ca^{2+}] in the nM range (109). However, Goll et al. (p757) recently reported that no proteolytic properties have

ever been attributed to p94 (60). One possibility is that intracellular [Ca^{2+}], in the present study, rose to a level sufficient to activate calpain, which then increased the α-fodrin breakdown reported here. The magnitude of calcium-activated fodrinolysis in ischemia-reperfusion injured cardiac tissue experiments is comparable to the present results, which supports the hypothesis that calpain is activated by increased [Ca^{2+}] after muscle damage (146).

While our data are consistent with the idea that the [Ca^{2+}] in damaged skeletal muscle fibers rises to levels sufficient to activate calpain (19), a second possibility is that muscle damage alters the sensitivity of calpain to Ca^{2+} activation. The autolysis of the 80 kDa and 28 kDa ubiquitous calpain subunits, in the presence of Ca^{2+}, to 78 kDa and 18 kDa respectively has been shown to decrease the half-maximal [Ca^{2+}] activation requirement by up to 8-fold (72). In keeping with this idea, Belcastro (18) found an exhaustive exercise-associated shift in calpain anion-exchange elution profile, which was interpreted to suggest calpain had autolyzed. This could explain his findings of a leftward shift in the *in vitro* half-maximal [Ca^{2+}] requirement for both u- and m-calpains (18). Calpain activity can also be modulated by a number of additional factors. These include intracellular redox conditions (63), calpastatin (an endogenous calpain inhibitor), cellular location (membrane proximity) (122), temperature, pH and phosphorylation status (143).

A final possibility is that muscle damage changed the susceptibility of α-fodrin to calpain degradation (64). Several myofibrillar proteins such as α-actinin,

tropomyosin, desmin and vimentin have been shown to be more susceptible to calpain-mediated degradation after exercise (18). Thus, our observation of elevated α-fodrin breakdown after damage could represent an increased susceptibility to degradation. Which of the above mechanisms, or combination of mechanisms, are responsible for the increased fodrinolysis under the *in vivo* conditions of the current study are not known but are currently under investigation in our laboratories.

Despite the long-standing interest in calpains and muscle damage, only a limited number of studies have examined calpain activity after contractile injury. As detailed above, Belcastro (18) found several indices of calpain activity had increased after exhaustive running exercise, but not all studies have found that calpain is active in injured muscle. Warren, et al. (154) recently concluded that calpain-mediated proteolysis was not responsible for the loss in P_o of skeletal muscles injured by lengthening contractions. This conclusion was based on the observation that the protease inhibitors leupeptin, calpeptin, and E-64d, failed to attenuate the decline in P_o that occurred immediately after lengthening contractions in mouse EDL. One possibility is that any contribution of calpain-mediated proteolytic activity to diminished force was masked by a much greater decrement caused by other mechanisms. Because histological and morphological alterations are observable in only 5-19% of muscle fibers after injury (52, 89), it seems likely that the major mechanism of functional decline immediately after injury is not caused exclusively by disruption of force-bearing structures. In fact, Ingalls et al. (71) ascribed 57-75% of the decrease in force after lengthening contractions to EC

coupling failure. In this regard, Papp et al. (112), showed that skinned cardiac myocytes (a preparation that by-passes EC coupling) incubated in m-calpain prior to test contractures had substantial decrements in force, which were correlated with ultrastructural alterations and desmin degradation Thus, the available evidence indicates that calpain degrades proteins necessary for force transmission. However, this does not appear to be the major mechanism of impairment after damage.

The current results show that calpain-mediated proteolysis is involved in the cellular response to injury that occurs after lengthening contractions. This could have several important consequences. First, it has been shown that the calpains cleave proteins associated with the stability of the thin and thick filaments, lateral force transmission and membrane stability in skeletal muscle (60). Titin, a known calpain substrate, spans the distance from the Z-line to the M-line. Its mechanical properties are primarily responsible for the force that is generated during passive lengthening (150). In addition, titin is credited with restoring stretched sarcomeres to their slack length, maintaining A-bands in their central position during contraction, and limiting length inhomogeneity in series-linked sarcomeres (67). Thus, calpain-induced damage to titin could promote the sarcomere popping proposed by Morgan.

Another protein identified as a potentially important calpain substrate is the intermediate filament protein desmin. Desmin connects Z-lines between myofibrils and is associated with lateral force transmission from the contractile proteins to the sarcolema. It has been well documented that immunostaining of the cytoskeletal-

protein desmin is diminished after lengthening contractile injury (89); however, injury-associated proteolysis of desmin has yet to be directly linked to *in vivo* calpain activity (15).

There is a well-documented inflammatory response to lengthening-contraction injury (48, 51) and this inflammatory response may be related to calpain activity (84). The peptide products of calpain cleavage are proposed to have a chemotactic role, which may stimulate inflammatory mechanisms and assist in the removal of damaged tissue (82, 117). Finally, it is now known that calpains are involved in cell signaling (125), gene regulation (11), and apoptosis (149), and that their activity is essential for cell survival (159). Thus, there is a wide range of normal and pathological mechanisms associated with calpains, which makes an understanding of their function imperative.

4.5.1. Summary and Conclusion

We found a significant increase in α-fodrin breakdown in EDL muscles injured by lengthening contractions. Because the fodrin breakdown products observed here are due to the activity of the neutral protease calpain, our results demonstrate that calpain-mediated proteolysis is increased after *in vivo* lengthening contraction-induced injury in EDL muscles of rat. This increase in calpain-mediated proteolysis may have important implications, not only in terms of sarcomere disassembly and degradation, but also for post-injury inflammation, gene expression, and cell survival.

CHAPTER 5

Summary

Kevin Marley

Department of Exercise and Sport Science

Our hypothesis was that calpains would be activated in exercise-injured skeletal muscle. Our aim was to test this idea using an *in vivo* model. To do this we needed to utilize a preparation that was controllable but also retained a reasonable degree of physiological relevance. Existing preparations described in the literature, such as downhill treadmill running or *in vitro* methods, proved to be either inadequately controllable, too expensive, or lacking in physiological relevance. Thus we set out to develop a new preparation.

The apparatus and methodology described in Chapter 3 represent a synthesis of ideas that were partially gleaned from the published literature, but mostly were developed using inexpensive and readily-available materials based on the maxim that necessity is the mother of invention. Using this system, we were able to study extensor digitorum longus muscles of rat that were exposed to passive-lengthening, active-isometric and active-lengthening contractions.

By measuring maximal isometric tetanic force before and after treatments, we were able to show that the active-lengthening contractions caused a significant decrement in the functional capacity of these muscles. Muscles exposed to control conditions showed no decrement in force, indicating that the lengthening contractions alone caused damage to these muscles. In addition, we used electron microscopy as a further measure of the extent of muscle damage caused by the lengthening-contraction protocol. After undergoing treatment, these muscles were then assayed for calpain-mediated proteolysis as described in Chapter 4. Briefly,

we quantified the appearance of specific peptide products of the breakdown of α-fodrin, a well accepted marker of calpain activity.

The unique results described in Chapter 4 are our findings of an increase in the 145 and 150 kDa peptides in exercise-injured muscles. Because these experiments were carried out using an *in situ* preparation, we interpreted the increase in these peptides as an up-regulation of calpain-mediated proteolysis under physiological conditions.

These findings are important because of the widespread nature of the function of calpain in biological mechanisms. Calpains are thought to play a key role in the normal turnover of proteins in cells. In addition they have been implicated in a number of pathologies, which include disuse muscle atrophy and muscular dystrophy but also such diverse diseases ranging from cataract disease to mental disorders. As such, knowledge of the functions and mechanisms of calpain has become imperative. In this regard, it seems unlikely that each of the many apparent functions of calpain operate by a unique mechanism. Rather, there are probably a limited number of mechanisms that generally apply across numerous conditions. Thus, an increased understanding of calpain function in injured skeletal muscle may provide useful insight in the functional mechanisms of calpain in other systems.

It has been well-established that muscle soreness and functional decline peak between 24 and 72 hours after injury. Protection from similar injury is transiently afforded to recovered muscles. Although these responses have been

well-documented, their mechanisms have not. We have shown that calpains are activated during the first hour following exercise-induced muscle injury. Although it does not appear that calpain-mediated proteolysis is the primary mechanism of force loss after damage, calpains are clearly active in these tissues and likely contribute in part to this functional decrement. In addition, calpains are suspected to be involved in the inflammatory response that follows injury. There are limited data that have shown that suppression of the inflammatory response also suppresses the recovery and protection that follows. Thus, the available evidence suggests calpains play a role in the mechanisms of muscle recovery after injury.

There has been a great deal of knowledge acquired recently concerning the function and regulation of calpain, yet there are a number of essential questions that require further investigation if an understanding of calpain is to be achieved. These include questions concerning: 1) how calpains are regulated under *in vivo* conditions; 2) the time-course of their activity after injury in skeletal muscle; and 3) their *in vivo* targets and the downstream consequences of their cleavage.

References

1. **Aidley DJ.** *The Physiology of Excitable Cells*: Cambridge University Press, 1998.

2. **Allen DG.** Eccentric muscle damage: mechanisms of early reduction of force. *Acta Physiologica Scandinavica* 171: 311-319, 2001.

3. **Allen DG, Lee JA, and Westerblad H.** Intracellular calcium and tension during fatigue in isolated single muscle fibres from *Xenopus laevis*. *Journal of Physiology (London)* 415: 433-458, 1989.

4. **Ariyoshi H, Shiba E, Sakon M, Kambayashi J, Yoshida K, Kawashima S, and Mori T.** Translocation of human platelet calpain-I. *Biochemistry and Molecular Biology International* 1: 63-72, 1993.

5. **Armstrong RB.** Initial events in exercise-induced muscle damage. *Medicine and Science in Sports and Exercise* 22: 429-435, 1990.

6. **Armstrong RB.** Mechanisms of exercise-induced delayed onset muscular soreness: a brief review. *Medicine and Science in Sports and Exercise* 16: 529-538, 1984.

7. **Armstrong RB, Duan C, Delp MD, Hayes DA, Glenn GM, and Allen DG.** Elevations in rat soleus muscle calcium with passive stretch. *Journal of Applied Physiology* 74: 2990-2997, 1993.

8. **Armstrong RB, Warren GL, and Warren JA.** Mechanisms of exercise-induced muscle fibre injury. *Sports Medicine* 12: 184-207, 1991.

9. **Arthur GD, Booker TS, and Belcastro AN.** Exercise promotes a subcellular redistribution of calcium-stimulated protease activity in striated muscle. *Canadian Journal of Physiology and Pharmacology* 77: 42-47, 1999.

10. **Ashton-Miller JA, Veerichetty YH, Kadhiresan VA, McCubbrey DA, and Faulkner JA.** An apparatus to measure *in vivo* biomechanical behavior of dorsi- and plantar flexors of mouse ankle. *American Physiological Society* 72: 1205-1211, 1992.

11. **Azam M, Andrabi SS, Sahr KE, Kamath L, and Kuliopulos A.** Disruption of the mouse mu-calpain gene reveals an essential role in platelet function. *Molecular and Cellular Biology* 21: 2213-2220, 2001.

12. **Bailey JL, Wang X, England BK, Price SR, Ding X, and E. MW.** The acidosis of chronic renal failure activates muscle proteolysis in rats by augmenting

transcription of genes encoding proteins of the ATP-dependent ubiquitin-proteasome pathway. *Journal of Clinical Investigation* 97: 1447-1453, 1996.

13. **Balnave CD and Allen DG.** The effect of muscle length on intracellular calcium and force in single fibres from mouse skeletal muscle. *Journal of Physiology (London)* 492: 705-713, 1996.

14. **Balnave CD, Davey DF, and Allen DG.** Distrubution of sarcomere length and intracelllular calcium in mouse skeletal muscle following stretch-induced injury. *Journal of Physiology (London)* 502: 649-659, 1997.

15. **Barash IA, Peters D, Fridén J, Lutz GJ, and Lieber RL.** Desmin cytoskeletal modifications after a bout of eccentric exercise in the rat. *American Journal of Physiology: Regulatory Integrative and Comparative Physiology* 283: R958-R963, 2002.

16. **Barondess J.** Musculoskeletal disorders and the workplace. Washington, D.C.: National Academy Press, 2001.

17. **Beaton L, Tarnopolsky M, and Phillips S.** Contraction-induced muscle damage in humans following calcium channel blocker administration. *Journal of Physiology* 544: 849-859, 2002.

18. **Belcastro AN.** Skeletal muscle calcium-activated neutral protease (calpain) with exercise. *Journal of Applied Physiology* 74: 1381-1386, 1993.

19. **Belcastro AN, Shewchuk LD, and Raj DA.** Exercise-induced muscle injury: a calpain hypothesis. *Molecular and Cellular Biochemistry* 179: 135-145, 1998.

20. **Berchtold MW, Brinkmeier H, and Müntener M.** Calcium ion in skeletal muscle: its crucial role for muscle function, plasticity, and disease. *Physiological Reviews* 80: 1215-1265, 2000.

21. **Best TM, McCabe RP, Corr D, and Vanderby R.** Evaluation of a new method to create a standardized muscle stretch injury. *Medicine and Science in Sports and Exercise* 30: 200-205, 1997.

22. **Booth J and Sutton JR.** Impaired calcium pump function does not slow relaxation in human skeletal muscle after prolonged exercise. *Journal of Applied Physiology* 83: 511-521, 1997.

23. **Branca D, Gugliucci A, Bano D, Brini M, and Carafoli E.** Expression, partial purification and functional properties of themuscle-specific calpain isoform p94. *European Journal of Biochemistry* 265: 839-846, 1999.

24. **Brooks SV and Faulkner JA.** Maximum and sustained power of extensor digitorum longus muscles from young, adult, and old mice. *Journal of Gerontology Biological Sciences* 46: B28-B33, 1991.

25. **Brooks SV, Zerba E, and Faulkner JA.** Injury to muscle fibres after single stretches of passive and maximally stimulated muscles of mice. *Journal of Applied Physiology*: 459-469, 1995.

26. **Bruton JD, Lännergren J, and Westerblad H.** Mechano-sensitive linkage in excitation-contraction coupling in frog skeletal muscle. *Journal of Physiology (London)* 484: 737-742, 1995.

27. **Bullard B, Sainsbury G, and Miller N.** Digestion of proteins associated with the Z-disk by calpain. *Journal of Muscle Research and Cell Motility* 11: 271-279, 1990.

28. **Byrd SK.** Alterations in the sarcoplasmic reticulum: a possible link to exercise-induced muscle damage. *Medicine and Science in Sports and Exercise* 24: 531-536, 1992.

29. **Byrd SK, McCutcheon L, Hodgson D, and P. G.** Altered sarcoplasmic reticulum function after high intensity exercise. *Journal of Applied Physiology* 67: 2072-2077, 1989.

30. **Carafoli E.** The homeostasis of calcium in heart cells. *Journal of Molecular and Cellular Cardiology* 17: 202-212, 1985.

31. **Carlson RC and Villarin JJ.** Membrane excitability and calcium homeostasis in exercising skeletal muscle. *American Journal of Physical Medicine and Rehabilitation* 81: S28-S39, 2002.

32. **Casella E.** Tensile force in total striated muscle, isolated fiber and sarcolemma. *Acta Physiologica Scandinavica* 21: 380-401, 1951.

33. **Clarkson PM.** Exercise-induced muscle damage, repair, and adaptation in humans. *Journal of Applied Physiology* 65: 1-6, 1988.

34. **Clarkson PM and Sayers SP.** Etiology of exercise-induced muscle damage. *Journal of Applied Physiology* 24: 234-248, 1995.

35. **Daddow L.** An abbreviated method of double lead staining. *Journal of Submicroscopy and Cytology* 18: 221-224, 1986.

36. **De Windt LJ, Willems J, Roemen TH, Coumans WA, Reneman RS, Van Der Vusse GJ, and Van Bilsen M.** Ischemic-reperfused isolated working

mouse hearts: membrane damage and type IIA phospholipase A2. *American Journal of Physiology Heart and Circulation Physiology* 280: H2572-H2580, 2001.

37. **Dear TN and Boehm T.** Diverse mRNA expression patterns of the mouse calpain genes Capn5, Capn6 and Capn11 during development. *Mechanisms of Development* 89: 201-209, 1999.

38. **Duan C, Delp MD, Hayes DA, Delp PD, and B. AR.** Rat skeletal muscle mitochondrial [Ca^{2+}] and injury from downhill walking. *Journal of Applied Physiology* 68: 1241-1251, 1990.

39. **Duncan CJ.** Role of calcium in triggering rapid ultrastructural damage in muscle: a study with chemically skinned fibres. *Journal of Cell Science* 87: 581-584, 1987.

40. **Duncan CJ.** The role of phospholipase A2 in calcium-induced damage in cardiac and skeletal muscle. *Cell and Tissue Research* 253: 457-462, 1988.

41. **Enoka RM.** Eccentric contractions require unique activation strategies by the nervous system. *Journal of Applied Physiology* 81: 2339-2346, 1996.

42. **Ervasti JM.** Costameres: the achilles' heal of herculean muscle. *Journal of Biological Chemistry* 278: 13591-13594, 2003.

43. **Faulkner JA, Jones DA, and Round JM.** Injury to skeletal muscles of mice by forced lengthening during contractions. *Quarterly Journal of Experimental Physiology* 74: 661-670, 1989.

44. **Feason L, Stockholm D, Freyssenet D, Richard I, Duguez S, Beckmann JS, and Denis C.** Molecular adaptations of neuromuscluar disease-associated proteins in response to eccentric exercise in human skeletal muscle. *Journal of Physiology (London)* 543.1: 297-306, 2002.

45. **Fitts RH.** Cellular mechanisms of muscle fatigue. *Physiological Reviews* 74: 49-94, 1994.

46. **Franco A and Lansman J.** Stretch-sensitive channels in developing muscle cells from a mouse cell line. *Journal of Physiology (London)* 427: 361-380, 1990.

47. **Fridén J.** Changes in human skeletal muscle induced by long-term eccentric exercise. *Cell and Tissue Research* 236: 365-372, 1984.

48. **Fridén J and Lieber RL.** Eccentric exercise-induced injuries to contractile and cytoskeletal muscle fibre components. *Acta Physiologica Scandinavica* 171: 321-326, 2001.

49. **Fridén J and Lieber RL.** Structural and mechanical basis of exercise-induced muscle injury. *Medicine and Science in Sports and Exercise* 24: 521-530, 1992.

50. **Fridén J and Lieber RL.** Subtle indications of muscle damage following eccentric contractions. *Acta Physiologica Scandinavica* 142: 523-524, 1991.

51. **Fridén J, Sfakianos PN, and Hargens AR.** Residual muscular swelling after repetitive eccentric contractions. *Journal of Orthopaedic Research* 6: 493-498, 1988.

52. **Fridén J, Sjöström M, and Ekblom B.** Myofibrillar damage following intense eccentric exercise in man. *International Journal of Sports Medicine* 4: 170-176, 1983.

53. **Furuno K and Goldberg AL.** The activation of protein degradation in muscle by Ca^{2+} or muscle injury does not involve a lysosomal mechanism. *Biochemical Journal* 237: 859-864, 1986.

54. **Furuno K, Goodman MN, and Goldberg AL.** Role of the different proteolytic systems in the degradation of muscle proteins during denervation atrophy. *Journal of Biological Chemistry* 265: 8550-8557, 1990.

55. **Gil-Parrado S, Popp O, Knoch TA, Zahler S, Bestvater F, Felgenträger M, Holloschi A, Fernández-Montalván A, Auerswald EA, Fritz H, Fuentes-Prior P, Machleidt W, and Spiess E.** Subcellular localization and in vivo subunit interactions of ubiquitous mu-calpain. *Journal of Biological Chemistry* 278: 16336-16346, 2003.

56. **Gissel H and Clausen T.** Excitation-induced Ca^{2+} influx and skeletal muscle cell damage. *Acta Physiologica Scandinavica* 171: 327-334, 2001.

57. **Gissel H and Clausen T.** Excitation-induced calcium uptake in rat skeletal muscle. *American Journal of Physiology Regulatory Integrative and Comparative Physiology* 276: R331-R339, 1999.

58. **Goll DE, Thompson VF, Taylor RG, Ouali A, and Chou RR.** The calpain system in skeletal muscle. In: *Calpain: Pharmacology and toxicology of calcium-dependent protease*, edited by Wang K and Yuen P. Ann Arbor: Taylor and Frances, 1999, p. 127-160.

59. **Goll DE, Thompson VF, Taylor RG, and Zalewska T.** Is calpain activity regulated by membranes and autolysis or by calcium and calpastatin? *BioEssays* 14: 549-556, 1992.

60. **Goll DE, Thompson VF, Wei Wei HL, and Cong J.** The calpain system. *Physiological Reviews* 83: 731-801, 2002.

61. **Gollnick P, Ianuzzo CD, Williams C, and Hill TR.** Effect of prolonged severe exercise on the ultrastructure of human skeletal muscle. *Int Z angew Physiol* 27: 257-265, 1969.

62. **Gordon AM, Huxley AF, and Julian FJ.** The variation in isometric tension with sarcomere length in vertebrate muscle fibres. *Journal of Physiology (London)* 184: 170-192, 1966.

63. **Guttman RP and Johnson G.** Oxidative stress inhibits calpain activity in situ. *Journal of Biological Chemistry* 273: 13331-13338, 1996.

64. **Harris AS and Morrow JS.** Calmodulin and calcium-dependent protease I coordinately regulate the interaction of fodrin with actin. *Proceedings of the National Academy of Science USA* 87: 3009-3013, 1990.

65. **Herzog W and Leonard TR.** Force enhancement following stretching of skeletal muscle: a new mechanism. *The Journal of Experimental Biology* 205: 1275-1283, 2002.

66. **Hill AV.** The dimensions of animals and their muscular dynamics. *Proceedings of the Royal Institute of Great Britain* 34: 450-471, 1950.

67. **Horowits R.** The physiological role of titin in striated muscle. *Nature* 323: 160-164, 1986.

68. **Hosfield CM, Ye Q, Arthur JS, Hegadorn C, Croall DE, Elce JS, and Jia Z.** Crystallization and X-ray crystallographic analysis of m-calpain, a Ca2+-dependent protease. *Acta Crystallogr D Biol Crystallogr* 8: 1484-1486, 1999.

69. **Huang J and Forsberg NE.** Role of calpain in skeletal-muscle protein degradation. *Proceedings of the National Academy of Science USA* 95: 12100-12105, 1998.

70. **Ikemoto M, Nikawa T, Takeda S, Watanabe C, Kitano T, Baldwin KM, Izumi R, Nonaka I, Towatari T, Teshima S, Rokutan K, and Kishi K.** Space shuttle flight (STS-90) enhances degradation of rat myosin heavy chain in association with activation of ubiquitin-proteasome pathway. *FASEB Journal* 15: 1279-1281, 2001.

71. **Ingalls CP, Warren GL, Williams JH, Ward CW, and Armstrong RB.** E-C coupling failure in mouse EDL muscle after in vivo eccentric contractions. *Journal of Applied Physiology* 85: 58-67, 1998.

72. **Inomata M, Hayashi M, Nakamura M, Saito Y, and Kawashima S.** Properties of erythrocyte membrane binding and autolytic activation of calpain. *Journal of Biological Chemistry* 264: 18838-18843, 1989.

73. **Jackson M, Jones D, and Edwards H.** Experimental muscle damage: the nature of the calcium activated degenerative processes. *European Journal of Clinical Investigation* 14: 369-374, 1984.

74. **Johnson G and Guttman RP.** Calpains: intact and active? *BioEssays* 19: 1011-1018, 1997.

75. **Jones DA, Jackson MJ, McPhail G, and Edwards RH.** Experimental mouse muscle damage: the importance of external calcium. *Clinical Science* 66: 317-322, 1984.

76. **Kandarian SC and Stevenson EJ.** Molecular events in skeletal muscle during disuse atrophy. *Exercise and Sport Science Reviews* 30: 111-116, 2002.

77. **Katz B.** The relationship between force and speed in muscular contraction. *Journal Physiology (London)* 96: 45-64, 1939.

78. **Kluck RM, Bossy-Wetzel E, Green DR, and Newmeyer DD.** The release of cytochrome-c from mitochondria: a primary site for Bcl-2 regulation of apoptosis. *Science* 275: 1132-1136, 1997.

79. **Koh TJ and Escobedo J.** Cytoskeletal disruption and small heat shock protein translocation immediately after lengthening contractions. *American Journal of Physiology: Cell Physiology* 286: C713-C722, 2004.

80. **Kuboki M, Ishii H, and Kazama M.** Characterization of calpain-1 binding proteins in human erythrocyte plasma membrane. *Journal of Biochemistry* 107: 776-780, 1990.

81. **Kumamoto T, Kleese WC, Cong J, Goll DE, Pierce PR, and Allen RE.** Localization of the Ca^{2+}-dependent proteinases and their inhibitor in normal, fasted, and denervated rat skeletal muscles. *Anatomical Record* 232: 60-77, 1992.

82. **Kunmatsu M.** Neutrophil responses induced by formyl and acetyl peptides with the n-terminal sequence of the calpain small subunit. *Biochemical and Molecular Biology International* 31: 477-484, 1993.

83. **Lamb GD, Junankar PR, and Stephenson DG.** Raised intracellular [Ca2+] abolishes excitation-contraction coupling in skeletal muscle fibres of rat and toad. *Journal of Physiology (London)* 489: 349-362, 1995.

84. **Lapointe BM, Frenette J, and Côté CH.** Lengthening contraction-induced inflammation is linked to secondary damage but devoid of neutrophil invasion. *Journal of Applied Physiology* 92: 1522-1601, 2002.

85. **Lecker SH, Solomon V, and Mitch WE.** Muscle protein breakdown and the critical role of the ubiquitin-proteasome pathway in normal and disease states. *Journal of Nutrition* 129: 227S-237S, 1999.

86. **Lieber RL and Fridén J.** Mechanisms of muscle injury after eccentric contraction. *Journal of Science and Medicine in Sport / Sports Medicine Australia* 2: 253-265, 1999.

87. **Lieber RL and Fridén J.** Muscle damage is not a function of muscle force but active muscle strain. *Journal of Applied Physiology* 74(2): 520-526, 1993.

88. **Lieber RL, Schmitz MC, Mishra DK, and Friden J.** Contractile and cellular remodeling in rabbit skeletal muscle after cyclic eccentric contractions. *Journal of Applied Physiology* 77: 1926-1934, 1994.

89. **Lieber RL, Thornell LE, and Fridén J.** Muscle cytoskeletal disruption occurs within the first 15 min of cyclic eccentric contraction. *Journal of Applied Physiology* 80: 278-284, 1996.

90. **Lieber RL, Woodburn TM, and Fridén J.** Muscle damage induced by eccentric contractions of 25% strain. *Journal of Applied Physiology* 70: 2498-2507, 1991.

91. **Lowe DA, Warren GL, Hayes DA, Farmer MA, and Armstrong RB.** Eccentric contraction-induced injury of mouse soleus muscle: effect of varying Ca^{2+}. *Journal of Applied Physiology* 76: 1445-1453, 1994.

92. **Lowe DA, Warren GL, Ingalls CP, Boorstein DB, and Armstrong RB.** Muscle function and protein metabolism after initiation of contraction-induced injury. *Journal of Applied Physiology* 79: 1260-1270, 1995.

93. **Lowell BB, Ruderman NB, and Goodman MN.** Evidence that lysosomes are not involved in the degradation of myofibrillar proteins in rat skeletal muscle. *Biochemical Journal* 234: 237-240, 1986.

94. **Lynch GS, Fary CJ, and Williams DA.** Quantitative measurement of resting skeletal muscle Ca^{2+} following acute and long-term downhill running exercise in mice. *Cell Calcium* 22: 373-383, 1997.

95. **Magid A, Law, D. J.** Myofibrils bear most of the resting tension in frog skeletal muscle. *Science* 230: 1280-1282, 1985.

96. **Matsumura Y, Saeki E, Inoue M, Hori M, Kamada T, and Kusuoka H.** Inhomogeneous disappearance of myofilament-related cytoskeletal proteins in stunned myocardium of guinea pig. *Circulation Research* 79: 447-454, 1996.

97. **Matsumura Y, Saeki E, Otsu K, Morita T, Takeda H, Kuzuya T, Hori M, and Kusuoka H.** Intracellular calcium level required for calpain activation in a single myocardial cell. *Journal of Molecular and Cellular Cardiology* 33: 1133-1142, 2001.

98. **McCully KK and Faulkner JA.** Injury to skeletal muscle fibres of mice following lengthening contractions. *Journal of Applied Physiology* 59: 119-126, 1986.

99. **McHugh MP, Connolly DAJ, Easton RG, and Gleim GW.** Exercise-induced muscle damage and potential mechanisms for the repeated bout effect. *Sports Medicine* 27: 157-170, 1999.

100. **Mishra DK, Fridén J, Schmitz MC, and Lieber RL.** Anti-inflammatory medication after muscle injury. A treatment resulting in short-term improvement but subsequent loss of muscle function. *Journal of Bone and Joint Surgery American Volume* 77: 1510-1519, 1995.

101. **Morgan DL.** New insights into the behavior of muscle during active stretching. *Biophysical Journal* 57: 209-221, 1990.

102. **Morgan DL and Allen DG.** Early events in stretch-induced muscle damage. *Journal of Applied Physiology* 87: 2007-2015, 1999.

103. **Moss RL.** Sarcomere length-tension relations of frog skinned musle fibres during calcium activation at short lengths. *Journal of Physiology (London)* 292: 177-192, 1979.

104. **Nelson WJ and Traub P.** Proteolysis of vimentin and desmin by the Ca^{2+}-activated proteinase specific for these intermediate filament proteins. *Molecular and Cellular Biology*: 1146-1156, 1983.

105. **Newham DJ, Jones DA, Ghosh G, and Aurora P.** Muscle fatigue and pain after eccentric contractions at long and short length. *Clinical Science* 74: 553-557, 1988.

106. **Newham DJ, McPhail G, Mills K, and Edwards RH.** Ultrastructural changes after concentric and eccentric contractions of human muscle. *Journal of the Neurological Sciences* 61: 109-122, 1984.

107. **Nosaka K, Sakamoto K, Newton M, and Sacco P.** How long does the protective effect on eccentric exercise-induced muscle damage last? *Medicine and Science in Sports and Exercise* 33: 1490-1495, 2001.

108. **Ogilvie R, Armstong R, Baird K, and Bottoms C.** Lesions in rat soleus muscle following eccentrically biased exercise. *The American Journal of Anatomy* 182, 1988.

109. **Ono Y, Shimada H, Sorimachi H, Richard I, Saido TC, Beckmann JS, Ishiura S, and Suzuki K.** Functional defects of a muscle-specific calpain, p94, caused by mutations associated with limb-girdle muscular dystrophy type 2A. *Journal of Biological Chemistry* 273: 17073-17078, 1998.

110. **Ordway GA, Neufer DP, Chin ER, and DeMartino G.** Chronic contractile activity upregulates the proteosome system in rabbit skeletal muscle. *Journal of Applied Physiology* 88: 1134-1141, 2000.

111. **Overgaard K, Lindstrøm T, Ingemann-Hansen T, and Clausen T.** Membrane leakage and increased content of Na^+ -K^+ pumps and Ca^{2+} in human muscle after a 100-km run. *Journal of Applied Physiology* 92: 1891-1898, 2002.

112. **Papp Z, Van der Velden J, and Stienen GJM.** Calpain-I induced alterations in the cytoskeletal structure and impaired mechanical properties of single myocytes of rat heart. *Cardiovascular Research* 45: 981-993, 2000.

113. **Pillay CS, Elliott E, and Dennison C.** Endolysosomal proteolysis and its regulation. *Biochemical Journal* 363: 417-429, 2002.

114. **Pontremoli S, Viotti PL, Michetti M, Salamino f, and Melloni E.** Identification of an endogenous activator of calpain in rat skeletal muscle. *Biochemical and Biophysical Research Communications* 171: 569-574, 1990.

115. **Proske M and Morgan DL.** Muscle damage from eccentric exercise: mechanism, mechanical signs, adaptation and clinical applications. *Journal of Physiology (London)* 537: 333-345, 2001.

116. **Publicover SJ, Duncan CJ, and Smith JL.** The use of A23187 to demonstrate the role of intracellular calcium in causing ultrastructural damage in mammalian muscle. *Journal of Neuropathology and Experimental Neurology* 37: 554-557, 1978.

117. **Raj DA, Booker TS, and Belcastro AN.** Sriated muscle calcium-stimulated cysteine protease (calpain-like) activity promotes myeloperoxidase activity with exercise. *Pflügers Archives -European Journal of Physiology* 435: 804-809, 1998.

118. **Rappaport L.** Ischemia-reperfusion associated myocardial contractile dysfunction may depend on Ca^{2+}-activated cytoskeletal protein degradation. *Cardiovascular Research* 45: 810-812, 2000.

119. **Rinard J, M. CP, Smith LL, and Grossman M.** Response of males and females to high-force eccentric exercise. *Journal of Sports Sciences* 18: 229-236, 2000.

120. **Romatowski J, Thompson LV, Yarasheski KE, and Fitts RH.** Effect of strength training on the contractile function of slow and fast fibers in 60-70 yr olds (abstract). *Medicine and Science in Sports and Exercise* 26: S215, 1994.

121. **Saido TC, Yokota M, Nagao S, Yamaura I, Tanis E, Tsuchiya T, Suzuki K, and Kawashima S.** Spatial resolution of fodrin proteolysis in postischemic brain. *Journal of Biochemistry* 268: 25239-25243, 1993.

122. **Salamino F, De Tullio R, Mengotti P, Viotti PL, E. M, and Pontremoli S.** Site directed activation of calpain is promoted by a membrane-associated natural activator protein. *Biochemical Journal* 290: 191-197, 1993.

123. **Samis JA and Elce JS.** Immunogold electron-microscopic localization of calpain I in human erythrocytes. *Thromb Haemostas* 61: 250-253, 1989.

124. **Sasaki S, Kikuchi T, Yumoto N, Yoshimura N, and Murachi T.** Comparative specificity and kinetic studies on porcine calpain I and calpain II with naturally occurring peptides and synethetic fluorgenic substrates. *Journal of Biochemistry* 259: 12489-12494, 1984.

125. **Sato-Kusubata K, Yajima Y, and Kawashima S.** Persistent activation of Gs-alpha through limited proteolysis by calpain. *Biochemical Journal* 347: 733-740, 2000.

126. **Schwane JA, Johnson SR, Vandenakker CB, and Armstrong RB.** Delayed-onset muscular soreness and plasma CPK and LDH activities after downhill running. *Medicine and Science in Sports and Exercise* 15: 51-56, 1983.

127. **Shiba E, Ariyoshi H, Yano Y, Kawasaki T, Sakon M, Kambayashi J, and Mori T.** Purification and characterization of a calpain activator from human platelets. *Biochemical and Biophysical Research Communications* 182: 461-465, 1992.

128. **Solomon V and Goldberg AL.** Importance of the ATP-ubiquitin-proteasome pathway in the degradation of soluble and myofibrillar proteins in rabbit muscle extracts. *Journal of Biological Chemistry* 271: 26690-26697, 1996.

129. **Sorichter S, Puschendorf B, and Mair J.** Skeletal muscle injury induced by eccentric muscle action: muscle proteins as markers of muscle fiber injury. *Exercise Immunology Review* 5: 5-21, 1999.

130. **Sorimachi H, Imajoh-Ohmi S, Emori Y, Kawasaki H, Ohno S, Minami Y, and Suzuki K.** Molecular cloning of a novel mammalian calcium-dependent protease distinct from both m- and μ-types. *Journal of Biological Chemistry* 264: 20106-20111, 1989.

131. **Sorimachi H, Kimura S, Kinbara K, Kazama J, Takahashi M, Yajima H, Ishiura S, Sasagawa N, Nonaka I, Sugita H, Maruyama K, and Suzuki K.** Structure and physiological functions of ubiquitous and tissue-specific calpain species. Muscle-specific calpain, p94, interacts with connectin/titin. *Advances in Biophysics* 33: 101-122, 1996.

132. **Sorimachi H, Kinbara K, Kimura S, Takahashi M, Ishiura S, sasagawa N, Sorimachi N, Shimada H, Tagawa K, Maruyama K, and Suzuki K.** Muscle-specific calpain, p94, responsible for limb girdle muscular dystrophy type 2A, associates with connectin through IS2, a p94-specific sequence. *Journal of Biological Chemistry* 270: 31158-31162, 1995.

133. **Spencer MJ, Lu B, and Tidball JG.** Calpain II expression is increased by changes in mechanical loading of muscle in vivo. *Journal of Cellular Biochemistry* 64: 55-66, 1997.

134. **Stauber WT, Clarkson PM, Fritz VK, and Evans WJ.** Extracellular matrix disruption and pain after eccentric muscle action. *Journal of Applied Physiology* 69: 868-874, 1990.

135. **Stephenson DG, Nguyen LT, and Stephenson GMM.** Glycogen content and excitation-contraction coupling in mechanically skinned muscle fibres of the cane toad. *Journal of Physiology (London)* 519: 177-187, 1999.

136. **Stupka N, Tarnopolsky MA, Yardley NJ, and Phillips SM.** Cellular adaptation to repeated eccentric exercise-induced muscle damage. *Journal of Applied Physiology* 91: 1669-1678, 1985.

137. **Sultan KR.** Calpain activity in fast and slow transforming and regenerating skeletal muscle. *American Journal of Physiology Cell Physiology* 279: C639-C647, 2000.

138. **Suzuki K, Sorimachi H, Yoshizawa T, Kinbara K, and Ishiura S.** Calpain: novel family members, activation and physiological function. *Biological Chemistry* 376: 523-529, 1995.

139. **Takekura H, Fujinami N, Nishizawa T, Ogasawara H, and Kasuga N.** Eccentric exercise-induced morphological changes in the membrane systems involved in excitation-contraction coupling in rat skeletal muscle. *Journal of Physiology* 533: 571-583, 2001.

140. **Talbot JA and Morgan DL.** The effects of stretch parameters on eccentric exercise-induced damage to toad skeletal muscle. *Journal of Muscle Research and Cell Motility* 19: 237-245, 1998.

141. **Talbot JA and Morgan DL.** Quantitative analysis of sarcomere non-uniformities in active muscle following a stretch. *Journal of Muscle Research and Cell Motility* 17: 261-268, 1996.

142. **Thomas G, Zarnescu D, Juedes A, Bales M, and Londergan A.** Drosophila ß-heavy-spectrin is essential for development. *Development* 125: 2125-2134, 1998.

143. **Thompson CJ and Goll DE.** Phosphorylation of the calpains (Abstract). *Molecular Biology of the Cell* 11: 386a, 2000.

144. **Thompson JL, Balog EM, Fitts RH, and Riley DA.** Five myofibrillar lesion types in eccentrically challenged, unloaded rat adductor longus muscle--a test model. *The Anatomical Record* 254: 39-52, 1999.

145. **Trombitás K, Greaser M, Labeit S, Jin JP, Kellermayer M, Helmes M, and Granzier H.** Titin extensibility in situ: entropic elasticity of permanently folded and permanently unfolded molecular segments. *The Journal of Cell Biology* 1440: 853-859, 1998.

146. **Tsuji T, Ohga Y, Yoshikawa Y, Sakata S, Abe T, Tabayashi N, Kobayashi S, Kohzuki H, Yoshida KI, Suga H, Kitamura S, Taniguchi S, and Takaki M.** Rat cardiac contractile dysfunction induced by Ca2+ overload: possible link to the proteolysis of alpha-fodrin. *American Journal of Physiology Heart and Circulatory Physiology* 281: H1286-H1294, 2001.

147. **Van Der Meulen JH, McArdle A, Jackson MJ, and Faulkner JA.** Contraction-induced injury to the extensor digitorum longus muscles of rats: the role of vitamin E. *Journal of Applied Physiology* 83: 817-823, 1997.

148. **Van Eyk JE, Powers F, Law W, Larue C, Hodges RS, and Solaro RJ.** Breakdown and Release of Myofilament Proteins During Ischemia and Ischemia/Reperfusion in Rat Hearts : Identification of Degradation Products and Effects on the pCa-Force Relation. *Circulation Research* 82: 261-271, 1998.

149. **Vanden Hoek TL, Qin Y, Wojcik K, Li C, Shao Z, Anderson T, Becker LB, and Hamann KJ.** Reperfusion, not simulated ischemia, initiates intrinsic apoptosis injury in chick cardiomyocytes. *American Journal of Physiology Heart and Circulatory Physiology* 284: H141-H150, 2003.

150. **Wang K, McCarter R, Wright J, Beverly J, and Ramirez-Mitchell R.** Regulation of skeletal muscle stiffness and elasicity by titin isoforms: a test of the segmental extension model of resting tension. *Proceedings of the National Academy of Science USA* 88: 7101-7105, 1991.

151. **Wang K, Yuen, P.** Calpain. Philadelphia: Taylor and Francis, 1999.

152. **Warren GL, Hayes DA, Lowe DA, and Armstrong RB.** Mechanical factors in the initiation of eccentric contraction induced injury in rat soleus muscle. *Journal of Physiology (London)* 464: 457-475, 1993.

153. **Warren GL, Hayes DA, Lowe DA, Williams JH, and Armstrong RB.** Eccentric contraction-induced injury in normal and hindlimb-suspended mouse soleus and EDL muscles. *Journal of Applied Physiology* 77: 1421-1430, 1994.

154. **Warren GL, Ingalls CP, and Armstrong RB.** Temperature dependency of force loss and Ca^{2+} homeostasis in mouse EDL muscle after eccentric contractions. *American Journal of Physiology: Regulatory Integrative and Comparitive Physiology* 282: R1122-R1132, 2001.

155. **Yeung EW, Balnave CD, Ballard HJ, Bourreau JP, and Allen DG.** Development of T-tubular vacuoles in eccentrically damaged mouse muscle fibres. *Journal of Physiology* 540: 581-592, 2002.

156. **Yi-wen C, Hubal M, Hoffman E, Thompson PD, and M. CP.** Molecular responses of human muscle to eccentric exercise. *Journal of Applied Physiology* 95: 2485-2494, 2003.

157. **Yoshida K.** Myocardial ischemia-reperfusion injury and proteolysis of fodrin, ankyrin and calpastatin. In: *Calpain methods and protocols*, edited by Elce JS. Totowa, NJ: Humana Press Inc, 2000, p. 267-275.

158. **Zerba E and Faulkner JA.** Injury after single stretches of passive and maximally activated whole muscles of anethesthetized mice. *Journal of Physiology (London)* 488: 459-469, 1993.

159. **Zimmerman U, Boring L, Pak J, Mukerjee N, and Wang K.** The calpain small subunit gene is essential: its inactivation results in embryonic lethality. *IUBMB Life* 50: 63-68, 2000.